ISSN 0280-5316
ISRN LUTFD2/TFRT--5745--SE

Control of Bacillus Subtilis Cultivations – Feeding Strategies and the Role of Anti-windup in Mid-ranging Control

Maria Karlsson

Department of Automatic Control
Lund Institute of Technology
May 2005

Department of Automatic Control
Lund Institute of Technology
Box 118
SE-221 00 Lund Sweden

Document name
MASTER THESIS

Date of issue
May 2005

Document Number
ISRNLUTFD2/TFRT--5745--SE

Author(s)
Maria Karlsson

Supervisor
Per Hagander at Automatic Control in Lund.

Sponsoring organization

Title and subtitle
Control of Bacillus Subtilis Cultivations – Feeding Strategies and the Role of Anti-windup in Mid-ranging control. (Reglering av Bacillus subtitlisodlingar)

Abstract
The first part of this thesis investigates if probing control can be applied to glucose feeding of the bacteria *Bacillus subtilis* producing the enzyme xylanase. The experimental work reveals unexpected results, where growth and cell/glucose yield are significantly lower in the feed phase than in the batch phase of
a fed-batch cultivation. The reason for this is still unclear, but some hypotheses are presented, mainly problems with the medium composition or changes in glucose and growth dynamics at low glucose concentrations. The probing feeding algorithm achieves the goal of maximum growth under the constraint of avoiding glucose accumulation, but still suffers from the problem of slow growth and low cell/glucose yield.
In the second part of the thesis it is examined whether anti-windup mechanisms should be included into a mid-ranging controller aimed to decrease temperature to handle saturation of oxygen transfer in bacteria cultivations. Simulations and analysis show that anti-windup has disadvantages in the mid-ranging control setting but may help to ensure stability for faster temperature control loops

Keywords

Classification system and/or index terms (if any)

Supplementary bibliographical information

ISSN and key title
0280-5316

ISBN

Language
English

Number of pages
60

Recipient's notes

Security classification

Contents

Acknowledgements

First, I would like to thank my enthusiastic and encouraging thesis supervisor, professor Per Hagander, for all help during the past months. At the Department of Biotechnology I would like to thank master thesis student Ulf Svensson and his supervisor, professor Olle Holst, for great cooperation and for contributing with lots of knowledge on fermentation and microbiology. Eva Palmqvist at Danisco presented us with an interesting and challenging problem that helped me bridge the gap between theoretical control and industrial applications. Stephane Velut was very helpful in explaining computer programs and simulation code. David Carlström was very kind to proof-read the report. Finally, I would like to thank Toivo for all his patience and support.

1. Introduction

Modern industrial production of proteins, such as insulin and human growth hormone, makes use of genetically engineered bacteria. Foreign DNA that codes for the desired protein is inserted into the bacterial genome. The bacteria can then be grown in bioreactors, and the product – the protein – can be extracted from the cultivation medium or disintegrated cells. Efficient production requires that the bacteria grow fast to high cell densities. The supply of oxygen and nutrients, the pH, and the temperature must be properly controlled on-line to provide a suitable environment for cell growth and protein synthesis.

1.1 Problem Statement

In this thesis, it is examined whether an existing control scheme – *probing control* [1] [10]– can be applied to cultivations of the organism *Bacillus subtilis* producing the enzyme xylanase. The goal of the probing control algorithm is to adjust the feed rate to keep the glucose concentration just below a critical point where production of undesirable byproducts starts. This is achieved using a standard sensor for dissolved oxygen, without direct measurement of the glucose concentration. The key idea of the algorithm is that byproduct formation is linked to a saturation in the respiratory capacity of the bacteria, that can be traced in the dissolved oxygen signal.

Xylanase is an enzyme that degrades the polysaccharide xylan found in cell walls of plants. The industrial applications range from bleaching of paper to food additives [3]. The project presented in this thesis was initiated by the Danish company Danisco that produces xylanase for use in the bakery industry to improve quality of baked products.

A limitation of the probing feeding strategy is the saturation of oxygen transfer in the bioreactor. To handle this limitation, a mid-ranging controller has been developed that decreases the temperature in order to avoid oxygen transfer saturation [10]. The second part of this thesis is devoted to further analysis of this approach, with the goal of determining whether anti-windup mechanisms should be incorporated into the mid-ranging controller.

The original intention of the work presented in this thesis was to apply the results on anti-windup for mid-ranging control in the *Bacillus subtilis* cultivations. Due to unexpected differences between the dynamics of the *Bacillus subtilis* cultivations compared to organisms previously studied, it was not possible to test the results on mid-ranging control experimentally within the scope of this thesis. The experimental work on *Bacillus subtilis* cultivations, and the theoretical work on anti-windup for mid-ranging control can thus be viewed as two separate entities with the common theme in the relation to the probing feeding algorithm.

1.2 Thesis Outline

The report begins with a presentation of necessary background information on bacteria cultivations, the probing control algorithm, and the mathematical model of the process that is used for analysis. Some remarks on the organism

Bacillus subtilis are also presented. The next section describes the methods used in the experimental work, and the obtained results. In the fourth section, some remarks on the experimental results are presented. Unexpected results are pointed out, and different hypotheses explaning these results are presented and evaluated. The fifth section presents the mid-ranging controller and the anti-windup scheme. In this section, a simplified, linearized model of the process is derived and used for analysis. The thesis concludes with a discussion of the results, the questions that remain unanswered, and some directions for future work.

2. Background

2.1 Characteristics of Bacteria

Bacteria are unicellular, prokaryotic organisms that reproduce asexually by binary fission. They generally range in size from 1 to $10\mu m$. Bacteria reproduce by dividing into two identical copies, and depending on the type of bacteria the generation time – the mean time for a cell to divide – may range from 20 minutes to 24 hours [7].

The DNA of bacteria consists of a single chromosome, shaped as a circular loop. Bacteria may also have extra pieces of circular DNA called plasmids. As in all organisms, the role of the DNA is to pass genetic material to the next generation, and to provide the code for protein synthesis within the cell. Recombinant DNA technology involves introducing a piece of foreign DNA that codes for a desired protein into the bacterial genome or the plasmid. Apart from the proteins necessary for growth, the cells will as a result produce the desired product.

Because bacteria reproduce by binary fission, they will grow exponentially in a cultivation, as long as nothing limits their growth. Growth may be limited by the lack of necessary nutrients or lack of dissolved oxygen in the cultivation medium, production of growth-inhibiting byproducts, or unsuitable temperatures or pH-levels.

There are a wide variety of different bacterial species that may be used in biotechnology processes. The most well-known is the species *Escherichia coli* that has several advantages as a host for recombinant protein production, such as a short generation time. *Bacillus subtilis* are rod-shaped bacteria that are also well studied. It is non-pathogenic and can consequently be used in the food industry. Another advantage of this organism is that it secretes the produced protein into the cultivation medium, which facilitates extraction of the product. The generation time is slightly longer than for *Escherichia coli*.

A protein is produced when the genes coding for that protein are active. The regulation of gene activity is an intricate process that is principally governed by two mechanisms: induction and repression. An inducible gene is active in presence of an inducer; a repressible gene is active in the absence of a repressor [9]. In the xylanase producing strain of *Bacillus subtilis*, xylanase production is repressed in the presence of the repressor glucose.

2.2 Cultivations of Bacteria

The objective of the cultivations is to make the bacteria grow fast and produce large amounts of high-quality protein, in a way that is economically efficient and gives reproducible results. The main phase of the cultivation takes place in a bioreactor. In order to use this equipment efficiently, the bacteria are first grown to sufficient cell densities in a shake flask before they are transferred to the reactor. The shake flask contains the bacteria in a liquid consisting of all necessary nutrients.

When the bacteria have reached sufficient cell denisities, they are transferred to the bioreactor where the main phase of the cultivation takes place. The bioreactor is a vessel, ranging in size from a couple of liters in laboratory scale to several cubic meters for industrial processes. The bioreactor contains the cells in the medium, which is a liquid that contains all nutrients necessary for growth.

In a stirred tank reactor, the medium is mixed by a mechanical stirrer that ensures oxygen transfer to the liquid phase as well as good mixing. The reactor must also have mechanisms for heating and cooling, inlet and outlet of gas, and equipment to add components during the cultivation and withdrawing of test samples in a way that preserves aseptic conditions. All equipment must be properly sterilized.

Two modes of operation are used in the experimental work presented in this thesis: batch mode and fed-batch mode. In batch mode, all components of the medium are added to the bioreactor at the start of the cultivation. If the cells are to be grown to high cell densities, batch-mode may not be feasible since some nutrients would be required in such high concentration that they limit growth at the start of the cultivation.

This problem is overcome using the fed-batch mode of cultivation. A limited amount of medium components are added at the onset of the cultivation. When these components are consumed, the required nutrients are added continuously at a growth-limiting rate.

The bioreactor must be equipped with appropriate sensors to monitor the cultivation and provide information for feedback control. Standard equipment includes sensors for measuring pH, temperature, the percentage of carbon dioxide and oxygen in the outlet gas, and the amount of dissolved oxygen in the cultivation medium.

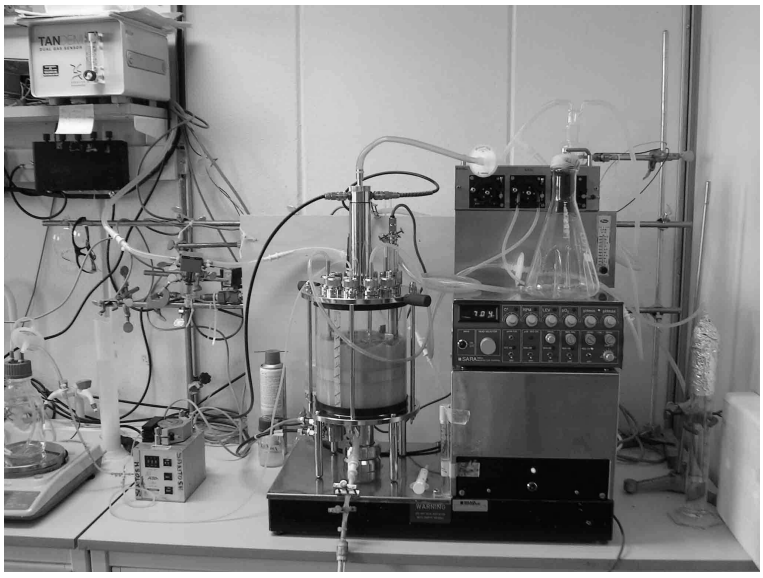

Figure 2.1 Bioreactor used in experimental work.

2.3 Dynamics of Bacterial Growth

Bacteria are the most simple form of living organisms. Even so, they demonstrate the complex, time-varying and to a certain extent unpredictable behavior representative of all living things. Some general models for the dynamics of bacterial growth can, however, be derived and verified experimentally. Such models are necessary in order to derive good control strategies, and to make simulations a useful tool in the analysis and synthesis of such control schemes.

A general dynamical model derived using mass and volume balances will be presented here [4]. This model has been experimentally verifed for the species *Escherichia coli*, and has been the background for developing the probing feeding algorithm. Here, the model is a starting point for finding a model of the *Bacillus subtilis* cultivations.

A rather extensive notation that will be used throughout the report is introduced in this section. An overview and summary is provided in table 2.3 at the end of the section.

Volume Dynamics

When the cultivation is run in fed-batch mode, a solution consisting of the substrate as well as other nutrients, the feed $F[l/h]$, is continuously added to the reactor. The volume $V[l]$ of the medium contained in the reactor will thus change according to

$$\frac{dV}{dt} = F. \tag{2.1}$$

Substrate Dynamics

All cells need energy for maintenance, reproduction, and synthesis of cell products to be transported out of the cell. The energy that the bacteria use come from some high-energy compound, called the substrate, provided in the medium. In the *Bacillus subtilis* cultivations, glucose was used as substrate.

The glucose uptake rate $q_g[g/gh]$ – the rate at which the cells consume glucose, is related to the glucose concentration $G[g/l]$. This relation is often modelled by the *Monod kinetics* model,

$$q_g(G) = q_g^{max}\frac{G}{k_s + G},$$

where q_g^{max} denotes the maximum uptake rate, and k_s is the saturation constant.

The rate of change of the total amount of glucose, VG, will equal the amount added through the feed minus the amount consumed by the cells, which is proportional to the total cell mass VX. We hence obtain the equation

$$\frac{d(VG)}{dt} = FG_{in} - q_g(G)VX, \tag{2.2}$$

where $G_{in}[g/l]$ is the glucose concentration in the feed.

The cells use glucose for four main purposes:

- maintenance
- growth
- formation of desired products

- formation of byproducts

A mathematical model can be derived for the glucose consumption for each of these purposes. It is important to note that this description is only a model, that it is constricted to well-defined cultivation conditions, and that it may not apply to the dynamics of *Bacillus subtilis*.

Part of the glucose uptake is used for maintenance, that is, energy-consuming processes that prevent cell death but do not contribute to cell growth and reproduction. The part of the glucose uptake q_g that is used for maintenance is denoted q_m. If the glucose uptake is lower than a critical value q_{mc}, all energy will be used for maintenance, according to

$$q_m = \min(q_g(G), q_{mc}).$$

Glucose is also required for cell growth, which is mainly an aerobic process that requires a sufficient level of dissolved oxygen in the medium. The rate of glucose uptake used for growth by aerobic processes is denoted q_{gg}^{ox}, and will be called the oxidative flow. When the glucose concentration exceeds a critical value, the oxygen uptake rate of the cells, q_o, saturates at q_o^{max}, wherefore not all glucose may be consumed by aerobic processes. Some of the glucose will then be used in anaerobic processes that contribute less to cell growth and instead lead to production metabolic byproducts such as acetate. The rate of glucose uptake for byproduct formation is denoted q_{gg}^{fe}, and will be called the fermentative flow. Even though the fermentative processes do increase growth, they are undesirable because the resulting byproducts have been reported to inhibit growth and protein production.

A yield coefficient $Y_{\alpha\beta}$ denotes either how many units of the product α that are obtained when one unit of the reactant β is consumed, or how many units of the reactant α that are consumed per unit of the reactant β. The following equations defines the oxidative and fermentative glucose flows, respectively:

$$q_{gg}^{ox} = \min((q_o^{max} - q_m Y_{om})/Y_{og}, q_g - q_m)$$

$$q_{gg}^{fe} = q_g - q_m - q_{gg}^{ox}.$$

Here, Y_{om} is the oxygen/glucose yield for maintenance metabolism, and Y_{og} is the oxygen/glucose yield for growth.

Byproduct Dynamics

At high glucose concentrations, the oxygen uptake of the cells will saturate, yielding $q_{gg}^{fe} > 0$, and the byproduct will be produced at a rate q_a^p according to

$$q_a^p = q_{gg}^{fe} Y_{ag}.$$

The concentration of the byproduct is denoted $A[g/l]$, and the rate of change of the amount of byproduct is directly proportional to the amount of cells VX, according to

$$\frac{d(VA)}{dt} = q_a(G, A)VX. \tag{2.3}$$

At glucose concentrations below the critical value where the oxygen uptake saturates, the full respiratory capacity of the cells is not used. Under these

conditions, the cells may consume the byproducts previously formed by aerobic processes to gain energy. This consumption is also proportional to the amount of cells VX. We then obtain

$$q_a(G, A) = q_a^p(G) - q_a^c(G, A),$$

where q_a^p is the byproduct production rate, and q_a^c is the byproduct consumption rate. The potential consumption is related to the byproduct concentration according to the Monod kinetics model

$$q_a^{c,pot}(A) = q_a^{c,max} \frac{A}{k_a + A}.$$

The byproduct consumption will then be

$$q_a^c = \min(q_a^{c,pot}, (q_o^{max} - q_{gg}^{fe} Y_{og} - q_m Y_{om})/Y_{oa}).$$

Oxygen Dynamics

Oxygen is required for glucose and byproduct consumption, and the oxygen uptake rate q_o is given by the equation

$$q_o = q_{gg}^{ox} Y_{og} + q_m Y_{om} + q_a^c Y_{oa}.$$

Oxygen is transferred to the medium by the mechanical stirrer, and the transfer rate is related to the stirrer speed $N[rpm]$ (revolutions per minute). The rate of change of the amount of dissolved oxygen, denoted C_o, is described by the equation

$$\frac{d(VC_o)}{dt} = K_L a(N) V (C_o^* - C_o) - q_o(G, A) VX. \tag{2.4}$$

Here, C_o^* is the maximum dissolved oxygen concentration in the medium and $K_L a(\cdot)$ the function describing the relation between the stirrer speed and the oxygen transfer capacity. Dissolved oxygen is generally given in percent of the maximum dissolved oxygen concentration, $O[\%]$, where O is related to C_o according to Henry's law

$$O = HC_o,\ H = 14000\% l/g.$$

Cell Growth Dynamics

Finally, the cell mass increases according to

$$\frac{d(VX)}{dt} = \mu(G, A) VX, \tag{2.5}$$

where the growth rate μ can be computed as

$$\mu = q_{gg}^{ox} Y_{xg}^{ox} + q_{gg}^{fe} Y_{xg}^{fe} + q_a^c Y_{xa}.$$

Both the oxidative flow, the fermentative flow and the consumption of byproducts contribute to growth. The critical glucose flow where the oxygen uptake saturates is denoted q_g^{crit}. The fermentative flow q_{gg}^{fe} is non-zero when q_g exceeds q_g^{crit}, and the acetate consumption is non-zero when q_g is below q_g^{crit} provided that acetate is present in the medium.

In the model presented, it is assumed that production of the desired protein does not influence growth.

Symbol	*Description*
$A[g/l]$	Byproduct concentration
$C_o[g/m^3]$	Dissolved oxygen concentration
$C_o^*[g/m^3]$	Saturation concentration of dissolved oxygen
$F[l/h]$	Feed
$G[g/l]$	Glucose concentration in reactor
$G_{in}[g/l]$	Glucose concentration in feed
$H[\%l/g]$	Henry's constant
$k_a[g/l]$	Saturation constant for byproduct uptake
$K_La(N)[h^{-1}]$	Function relating stirrer speed to oxygen transfer
$k_s[g/l]$	Saturation constant for glucose uptake
$N[rpm]$	Stirrer speed
$O[\%]$	Dissolved oxygen concentration
$q_a[g/gh]$	Net byproduct uptake
$q_a^c[g/gh]$	Byproduct consumption
$q_a^{c,max}[g/gh]$	Maximum byproduct consumption
$q_a^{c,pot}[g/gh]$	Potential byproduct consumption
$q_a^p[g/gh]$	Byproduct production
$q_g[g/gh]$	Glucose uptake
$q_g^{crit}[g/gh]$	Maximum oxidative glucose uptake
$q_g^{max}[g/gh]$	Maximum glucose uptake
$q_{gg}^{fe}[g/gh]$	Oxidative glucose uptake
$q_{gg}^{ox}[g/gh]$	Fermentative glucose uptake
$q_m[g/gh]$	Glucose uptake for maintenance
$q_{mc}[g/gh]$	Maximum glucose uptake for maintenance
$q_o[g/gh]$	Oxygen uptake
$q_o^{max}[g/gh]$	Maximum glucose uptake
$V[l]$	Volume of medium
$X[g/l]$	Biomass concentration
$Y_{ag}[g/g]$	Byproduct / glucose yield
$Y_{oa}[g/g]$	Oxygen / byproduct yield
$Y_{og}[g/g]$	Oxygen / glucose yield for growth
$Y_{om}[g/g]$	Oxygen / glucose yield for maintenance
$\mu[h^{-1}]$	Cell growth

Table 2.1 Overview of notation.

2.4 Probing Control of Substrate Feeding

An adequate control algorithm for the bacteria cultivations should not require an exact model of the process. The parameters in the model are generally hard to determine experimentally, and vary substantially depending on cultivation

conditions such as temperature, pH, and composition of the medium. They also vary during the course of a cultivation, between different cultivations, and are specific to each bacterial species, or even to each strain of a particular species. The model presented in section 2.3 is complex, nonlinear, and many variables of interest for control cannot be measured online using standard instrumentation.

The goal of the probing feeding strategy is to maximize growth while avoiding production of metabolic byproducts that are formed at high glucose concentrations.

Production of metabolic byproducts is undesirable because they may inhibit both growth and protein production. The goal of the substrate feeding is to keep the glucose level just below the critical point where the respiratory capacity of the cells saturates and byproduct formation starts. Probing control uses the characteristic relation between the glucose flow and the oxygen flow in the reactor demonstrated in figure 2.2.

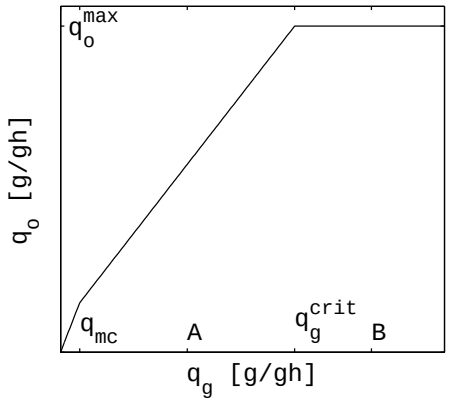

Figure 2.2 Oxygen uptake q_o as a function of glucose uptake q_g according to model in section 2.3.

The feed F should be chosen such that the glucose concentration is kept at a value G^{crit} corresponding to a glucose flow q_g just below q_g^{crit}. The glucose concentration cannot be measured online using standard sensors. Therefore, the critical glucose concentration should preferably be detected using standard instrumentation, such as a sensor for dissolved oxygen. Increasing the feed rate F will increase glucose concentration and thus the glucose flow rate q_g. If the original glucose flow was below the critical value q_g^{crit} at point A in figure 2.2, an increase in q_g will lead to an increase in the oxygen flow q_o. If the stirrer speed is kept constant, the dissolved oxygen level will subsequently decrease according to equation 2.4. If the original glucose flow was above the critical value, at point B in the figure, an increase in q_g will not give any response in the dissolved oxygen signal.

The probing control scheme presupposes a well-tuned PID-controller for keeping a constant dissolved oxygen level by adjusting the stirrer speed. The algorithm can be summarized as follows:

Pulse

- Freeze the stirrer speed at a constant value.
- Overload a pulse to the initial feedrate.

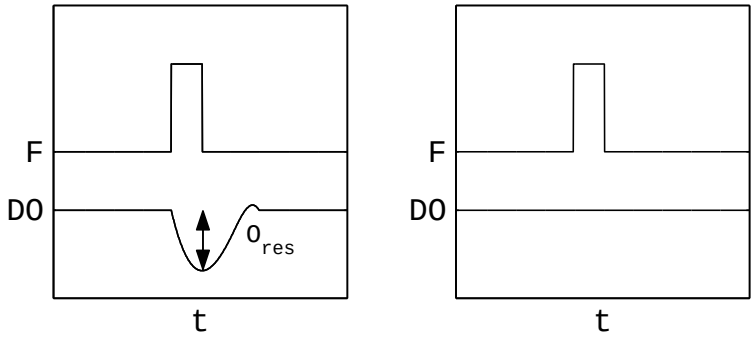

Figure 2.3 Pulse responses in dissolved oxygen signal at initial glucose flow $q_g < q_g^{crit}$ (left), and $q_g > q_g^{crit}$ (right)

- Measure the dissolved oxygen signal at the end of the feed pulse.
- If no response is seen in the oxygen signal, decrease the feed.
- If the dissolved oxygen decreases during the feed pulse, increase the feed.

Between pulses

- Keep the feed constant and keep the dissolved oxygen level at the setpoint by varying the stirrer speed until the next pulse.

According to the model, the closer the glucose uptake is to the critical value q_g^{crit}, the smaller will the response on feed pulses, O_{res}, be. Therefore, the magnitude of the pulse response, O_{res}, can be used for feedback to determine the change in feed F. A setpoint y_r for the oxygen response O_{res} is introduced. The setpoint should correspond to a suitable deviation from the critical glucose flow. In a region around y_r, the change in feedrate is given by the equation

$$\Delta F = \frac{\kappa}{O^* - O_{sp}} O_{res} F.$$

The relative change in the feedrate as a function of the pulse response is shown in figure 2.4.

The parameters that must be chosen in the control algorithm are listed in table 2.4. Guidelines for tuning are presented in [1].

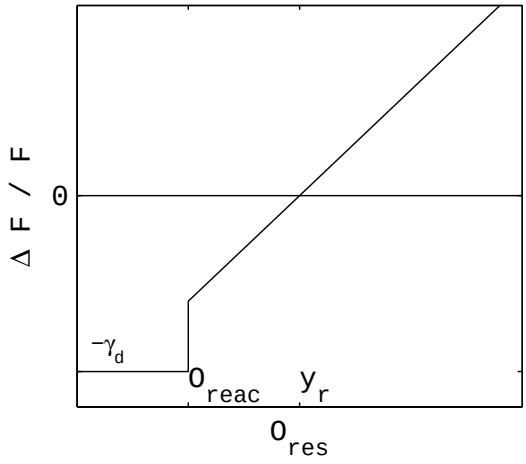

Figure 2.4 Relative change in feed, $\Delta F/F$ as a function of pulse response O_{res}

Parameter	*Description*
T_{pulse}	Pulse length
$T_{control}$	Time between pulses
O_{sp}	Setpoint for dissolved oxygen between pulses
O_{tol}	Pulse is delayed until the dissolved oxygen satisfies $\|O - O_{sp}\| \leq O_{tol}$
O_{reac}	For pulse responses below O_{reac}, F is decreased by a constant value
y_r	Reference value for pulse response
γ_d	Decrease in feedrate for pulse responses below O_{reac}
γ_p	Relative increase in F during the pulse
κ	Gain in the proportional part of the feed control

Table 2.2 Parameters in probing controller

3. Experimental Work

The purpose of the *Bacillus subtilis* cultivations is to produce the protein xylanase. Therefore, the goal of the work presented in this thesis is to find cultivation conditions that maximize protein production. Since production is related to cell density, a more direct goal has been to maximize cell growth.

Initially, the focus of the experimental work was to find a balanced medium composition to ensure that glucose was the limiting substance. This work is not central from a control engineering point of view and only a summary will be presented here, for a more detailed description see [8]. When satisfactory results were obtained in batch cultivations, the focus moved over to finding an appropriate feeding strategy to maximize growth in fed-batch cultivations.

In the first fed-batch cultivation, a fixed exponential feed profile was applied. In the following cultivations, feed profiles with different growth rates were tested. Feed pulses, where the feed was increased by 15% for periods of $90 - 120s$ were overloaded to the exponential feed rate, with constant stirrer speed during the pulses. Finally, the full probing control-algorithm was tested.

Because the results in the *Bacillus subtilis* cultivations do not match the model presented in section 2.3, some hypotheses explaining the deviation from the model have been suggested. These hypotheses are presented and discussed in section 4.

3.1 Equipment and Methods

The cultivations were performed in a $3l$ bio-reactor. The initial medium volume varied between 2 and $2.5l$ between the cultivations. Sensors were used to measure the pH, the temperature, and the dissolved oxygen level in the bioreactor, as well as oxygen and carbon dioxide content in the outlet gas from the reactor online. Samples were taken regularly for offline analysis of glucose concentration, cell dry weight, xylanase concentration, and optical density (OD). Optical density is a measure of how much light of a given wave length (here $600nm$) is absorbed by a test sample of the medium, and it is a convenient way of estimating cell density.

The temperature was kept constant, at 35^oC throughout the cultivations. Oxygen was transferred to the cultivation medium by the mechanical stirrer, and the dissolved oxygen level was kept at the reference value, $O = 30\%$, by a PID controller for the stirrer speed. To ensure good mixing, the stirrer speed was not allowed to decrease below $250rpm$. The pH was controlled to the reference value 7.0 by titration with ammonia. Under favorable growth conditions, the bacteria should not produce any products that increase the pH, therefore no acidic compound to decrease the pH was used.

The bacteria were pre-cultivated in shake flasks. Their growth rate during this period was monitored, so that they could be transferred to the bioreactor at a stage of exponential growth. The cell concentration at the start of the cultivation in the reactor was generally just below $1g/l$.

The cultivation medium was designed to provide a balance of all nutrients required for the desired final cell density. Apart from the substrate, glucose, the medium contained amino acids, salts, trace elements, and the antibiotic kanamycin. The bacterial strain that was used is resistant to kanamycin, and

as a consequence addition of this antibiotic prevents competition from other microorganims. For a detailed description of medium composition, see [8].

In the fed-batch cultivations, the feed starts when all initial glucose from the batch-phase is consumed. The exact time for this event is detected in the dissolved oxygen signal that increases rapidly when there is no glucose available, and the bacteria as a consequence do not consume any oxygen.

3.2 Batch Cultivation

Conditions The first cultivations were run in batch-mode, with all medium components added at the start of the cultivation. Different media were tested, varying with respect to concentrations of salts, glucose, and amino acids.

Aim The objective of these cultivations was to find a balanced cultivation medium, where glucose was the limiting substance. Another goal was to determine which specific growth rate μ that could be obtained, and to verify that the mathematical model in section 2.3 could be applied to this organism.

Results The batch cultivations could typically be divided into three stages. First there was a lag phase without substantial growth and without any significant changes in the dissolved oxygen, the glucose concentration or the composition of the outlet gas. This behavior is common in bacteria cultivations [4], and is a result of adaptation to the cultivation medium.

Second, there was a phase of exponential growth, with a corresponding exponential decline in the glucose concentration. During this phase the dissolved oxygen level decreases, and when it reaches the set point 30% the stirrer speed starts to increase. The concentration of carbon dioxide in the outlet gas also increases exponentially. This phase fits well with the mathematical model. The growth rate estimated from the carbon dioxide data was $\mu = 0.26h^{-1}$.

Third, after a period of exponential growth, the growth rate decreases into a linear pattern. At the same time, the stirrer speed settles at a value around $300rpm$. The carbon dioxide concentration also settles at a constant value, indicating a constant absolute growth rate. This change in dynamics comes at glucose concentrations well above zero. The third phase cannot be predicted using the existing model. Typical behavior in the second and third phases is shown in figure 3.1.

When all glucose is consumed, an instant and clear reaction can be seen in the data, see figure 3.2. The glucose uptake q_g decreases to zero, which causes the oxygen uptake q_o to be zero as well. When no oxygen is consumed, the stirrer speed decreases to its minimum value, and the carbon dioxide concentration also decreases, indicating that growth stops.

Conclusions A possible explanation for the onset of the third phase in the cultivation is that some substance in the medium other than glucose was limiting. When this substance is consumed, the metabolism of the cells somehow change to function without the missing substance, which explains the sudden change in dynamics.

The instant increase in dissolved oxygen when all glucose is consumed allows for rapid detection of glucose limitation. The increase in dissolved oxygen can consequently be used to start the glucose feed in fed-batch cultivations.

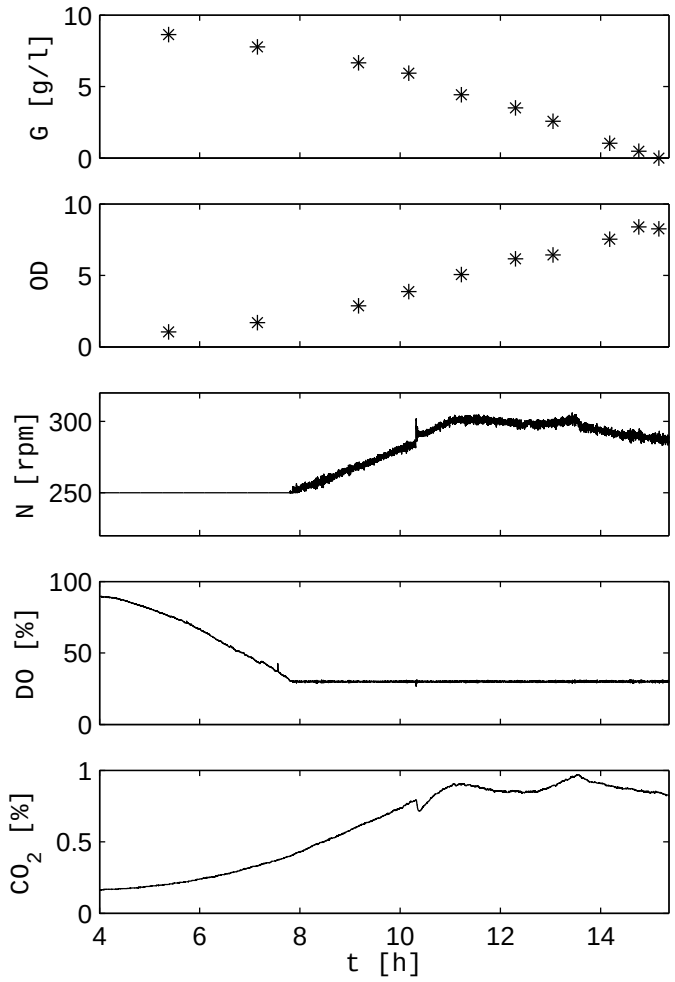

Figure 3.1 Glucose concentration, optical density, stirrer speed, dissolved oxygen, and carbon dioxide concentration in batch cultivation. The sudden change in the stirrer speed and carbon dioxide at $t = 10.5h$ is caused by addition of anti-foam.

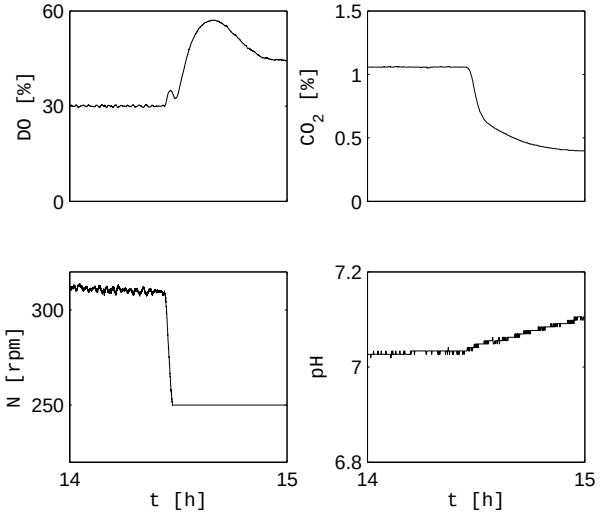

Figure 3.2 Response in dissolved oxygen, carbon dioxide, stirrer speed and pH when the glucose concentration reaches $G = 0$.

3.3 Response on Glucose Pulses

Conditions Glucose was injected into the medium at two occasions in the final stage of a batch cultivation. The first injection ($1.5g$ glucose), was made at glucose concentration approximately $G = 1g/l$, the second ($1g$ glucose) when all glucose had been consumed.

Aim The purpose of this experiment was to examine the impulse response from the input G to output O in figure 3.3, at two different glucose concentrations. Ultimately, this experiment was used to verify the saturation of the oxygen uptake q_o with respect to glucose uptake q_g, which allows for estimation of G from measurements of the dissolved oxygen concentration O.

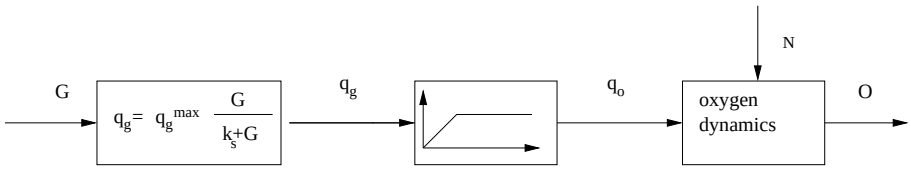

Figure 3.3 Relation between glucose concentration and dissolved oxygen.

Results The responses in the stirrer speed and dissolved oxygen on the glucose pulses are shown in figure 3.4.

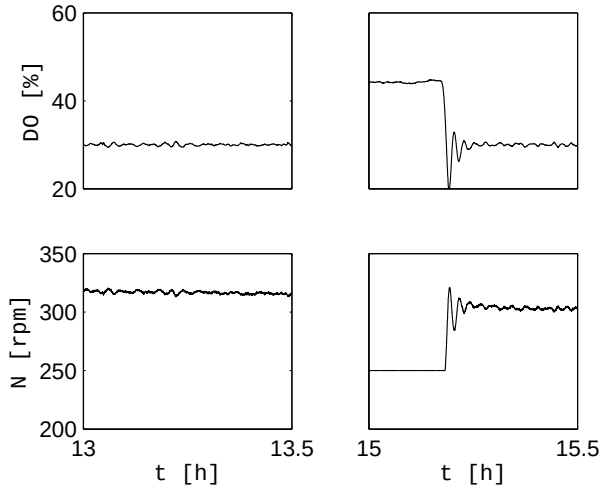

Figure 3.4 Impulse response from feed F to dissolved oxygen O when $G = 1g/l$ (left) and $G = 0g/l$ (right).

The amounts of glucose injected are relatively large. In the second experiment, the injected glucose immediately leads to saturation of the oxygen uptake, wherefore the dissolved oxygen and stirrer speed appear constant during the rest of the experiments.

Conclusions It is clear that the impulse response from a feed pulse to the dissolved oxygen signal depends on the initial glucose concentration. Glucose excess is linked to a saturation in oxygen uptake, so that an increase in substrate does not lead to any response in the oxygen signal.

3.4 Fed-batch Cultivation with Exponential Feed

Conditions The batch phase of the cultivation was run in the same manner as the previous cultivations. The medium was analyzed with respect to the need for different elements in the desired final cell density. The objective was to ensure that glucose would be the limiting substance.

A feed pump was started when a rapid increase in the dissolved oxygen signal, above $O = 50\%$, was observed, indicating that all glucose had been consumed. The feed contained glucose at concentration $100g/l$, amino acids, and kanamycin. The feed rate increased exponentially, according to

$$F = F_0 e^{\mu_f t}.$$

The feed increase rate $\mu_f = 0.05h^{-1}$ was chosen well below the maximum cell growth rate $\mu = 0.26h^{-1}$ observed in the batch cultivations. The initial feed flow F_0 was chosen to give an equilibrium point in the equation for the glucose dynamics

$$\frac{d(VG)}{dt} = FG_{in} - q_g(G)VX,$$

at time t_0, the feed start. An equilibrium point in this equation will prevent glucose accumulation, and give a feed F that matches the energy required for cell growth with a growth rate μ.

Assuming that $q_{gg}^{ox} \gg q_m$, $q_{gg}^{ox} \gg q_a^c$, and $q_{gg}^{fe} = 0$, we have

$$\mu = q_g Y_{xg}^{ox}.$$

The inital flow rate, at time t_0 can thus be computed as

$$F_0 = \frac{\mu V(t_0)X(t_0)}{G_{in}Y_{xg}^{ox}}. \tag{3.1}$$

From the previous batch cultivations, the parameter values could be approximated as $V(t_0)X(t_0) = 5g$ and $Y_{xg} = 0.3g/g$. The glucose concentration of the feed was $G_{in} = 100g/l$, and the desired growth rate $\mu = 0.05h^{-1}$, yielding $F_0 = 0.0083l/h$.

Aim The goal was to ensure that growth could continue in fed-batch mode, and to examine whether an exponential feed profile of growth rate $\mu_f = 0.05h^{-1}$ would lead to a corresponding growth in cell density.

Results The data from the cultivation is shown in figure 3.5.

The cultivation starts with a long lag-phase, $t = 0h-8h$, where the pH rises, and growth and glucose consumption are very low. The next phase, $t = 8h-20h$ shows characteristic exponential growth, with growth rate $\mu = 0.26h^{-1}$.

At $t = 20h$, both the stirrer speed and the carbon dioxide signal starts declining. This indicates a change in the system dynamics, that occurs before all glucose is consumed.

The sharp peak in the dissolved oxygen signal at $t = 21h$ indicates that all glucose has been consumed. The feed starts and the dissolved oxygen decreases immediately, despite the glucose flow being as low as $F = 0.0083l/h$. During the feed phase, growth is low. A growth rate of $\mu = 0.039h^{-1}$ can be observed in the carbon dioxide data in this phase. No glucose accumulation can be seen during the feed phase.

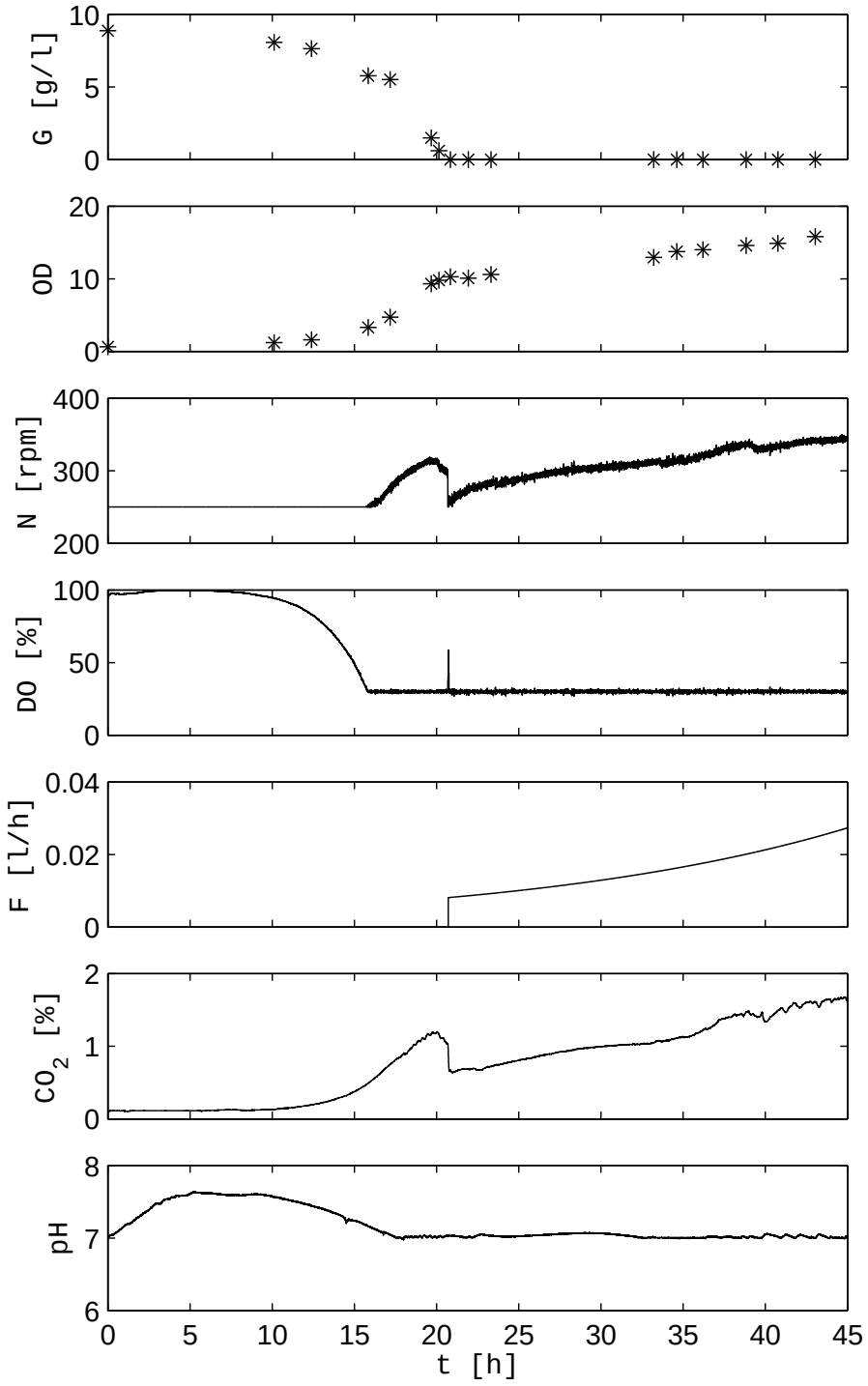

Figure 3.5 Fed-batch cultivation with exponential feed. From top: glucose concentration G, optical density OD, stirrer speed N, dissolved oxygen DO, feed F, pH, carbon dioxide in outgas CO_2, pH. The pH increases during the lag phase ($t = 0{-}8h$). The dissolved oxygen decreases during the exponential phase ($t = 8 - 20h$) until it reaches the set point $O = 30\%$. The exponential feed starts at $t = 21h$.

The glucose/cell dry weight yield Y_{xg} was 0.22 in the batch phase, and 0.08 in the feed phase.

Conclusions An exponential feed profile F with growth rate μ_f should asymptotically give rise to the same cell growth rate. A possible explanation for why the exponential feed rate $\mu_f = 0.05h^{-1}$ lead to a lower cell growth rate is that the adaptation rate is very slow. If the initial feed flow is chosen too low, the time it takes for the cell growth to reach the same exponential growth rate is much longer than the cultivation time.

No glucose is accumulated, and yet the cell/substrate yield is much lower in the batch phase. Possible explanations include that maintenance metabolism requires a higher relative glucose flow at lower glucose concentrations, and that xylanase production starts, taking energy from growth. This will be further discussed in the next section.

3.5 Response on Feed Pulses Overloaded on Exponential Feed

The use of the probing feeding strategy in cultivations of *Bacillus subtilis* ultimately depends on whether byproduct formation caused by excess glucose can be observed in the dissolved oxygen signal when the feed is perturbed by pulses. The impulse response experiments in section 3.3 demonstrated that injection of relatively large amounts of glucose can be used to detect whether the glucose flow is zero or is above the critical point q_g^{crit}. The probing feeding algorithm requires that the critical glucose flow can be detected by small increments in the feed rate, in the order of 20%.

Conditions To test the response on small feed increments, an exponential feed was applied, similarly as in the previous section. Two different cultivations were run using the same methods. In each cultivation, two different sets of feed growth rates μ_f were tested. In the first cultivation, $\mu_f = 0.03h^{-1}$ was applied for the first 14 hours, and $\mu_f = 0.06h^{-1}$ for the next 9 hours. In the second cultivation, $\mu_f = 0.06h^{-1}$ was used for the first 7 hours, and $\mu_f = 0.04h^{-1}$ for the next 15 hours.

In the first cultivation, the initial feed rate was computed according to (3.1). In the second cultivation, an attempt to compensate for maintenance metabolism was made. A more realistic model of the cell growth rate μ is

$$\mu = (q_g - q_m)Y_{xg}^{ox}.$$

If a cell growth rate of μ is desired, the initial feed rate required when maintenance is not negligible will be

$$F_0 = \frac{(\mu + q_m Y_{xg}^{ox})V(t_0)X(t_0)}{G_{in}Y_{xg}}.$$

The constant $q_m Y_{xg}^{ox}$ was estimated to $0.028h^{-1}$ from the result of the previous cultivations.

In both cultivations, when μ_f was changed, the new initial feed rate F_0 was computed with the expected cell density assuming the same cell growth rate

as feed increase rate, $\mu = \mu_f$, in the previous phase. From offline analysis of cell dry weight, it could be concluded that the actual cell densities were lower.

The feed was regularly increased by 15% for periods of $90 - 120s$. During these feed pulses, the stirrer speed was freezed at a constant value, and the response in the dissolved oxygen signal was observed.

Aim The purpose of these experiments was to verify that small increments in the feed, i.e. pulses, would give a reaction in the dissolved oxygen signal. It is also important to verify that the magnitude of these responses could be linked to the glucose concentration. Another goal was to gain sufficient information on the pulse responses to be able to tune the probing controller.

Different feed increase rates were tested to gain information on which cell growth rates that could be achieved in the feed-phase of a fed-batch cultivation, and how this is linked to glucose accumulation.

Results The results during the feed phases of both cultivations are shown in figure 3.6.

At the end of the batch-phase, the carbon dioxide concentration and the stirrer speed starts declining before all glucose is consumed. When all glucose is consumed, the oxygen signal increases rapidly. When it exceeds 50%, the feed is started.

In the first cultivation, the feed rate $\mu_f = 0.03h^{-1}$ gave a negligible cell growth rate, that is $\mu \approx 0h^{-1}$, and the feed rate $\mu_f = 0.06h^{-1}$ gave a cell growth rate of $\mu = 0.08h^{-1}$. The bacteria did not consume all glucose added in the last phase, so the glucose concentration increased to approximately $2g/l$. The initial feed rate for the period with $\mu_f = 0.06h^{-1}$ was adjusted to the expected cell density assuming a growth rate of $\mu = 0.03h^{-1}$ in the previous period. It is thus possible that the new glucose feed rate exceeded the critical glucose uptake rate. The growth rates are estimated from the carbon dioxide data.

In the second cultivation, the initial feed rate F_0 was chosen to compensate for maintenance metabolism. In the first period, the feed rate was $\mu_f = 0.06h^{-1}$ which gave a cell growth of $\mu = 0.02h^{-1}$. Some glucose accumulation can be seen at the end of this period. When the feed rate is decreased to $\mu_f = 0.04h^{-1}$, the accumulated glucose is consumed, and the cell growth rate is $\mu = 0.03h^{-1}$.

The oxygen responses at the end of the glucose pulses, $O_{res} = O_{sp} - O$ are shown in figure 3.7. The magnitude of the pulse responses are small, and the process noise is not negligible. However, on average, the impulse responses whithout measurable glucose accumulation are larger than with glucose accumulation, $O_{res} = 0.92$ compared to $O_{res} = 0.13$.

The stirrer speed and the dissolved oxygen demonstrate relatively large variance, especially towards the end of the second cultivation. It is likely that the PID-controller for the stirrer speed can be better tuned for the current operating range.

Conclusions Growth is much lower in the feed phase than in the batch phase. The critical feed rate that can be applied without glucose accumulation lies in the range $\mu = 0.04 - 0.06h^{-1}$. This corresponds to cell growth rates well below what can be achieved in the batch phase, where the cell growth rate has been approximately $\mu = 0.26h^{-1}$. For this organism, it appears that the critical growth rate is substantially lower than the maximum growth rate seen in the batch phase.

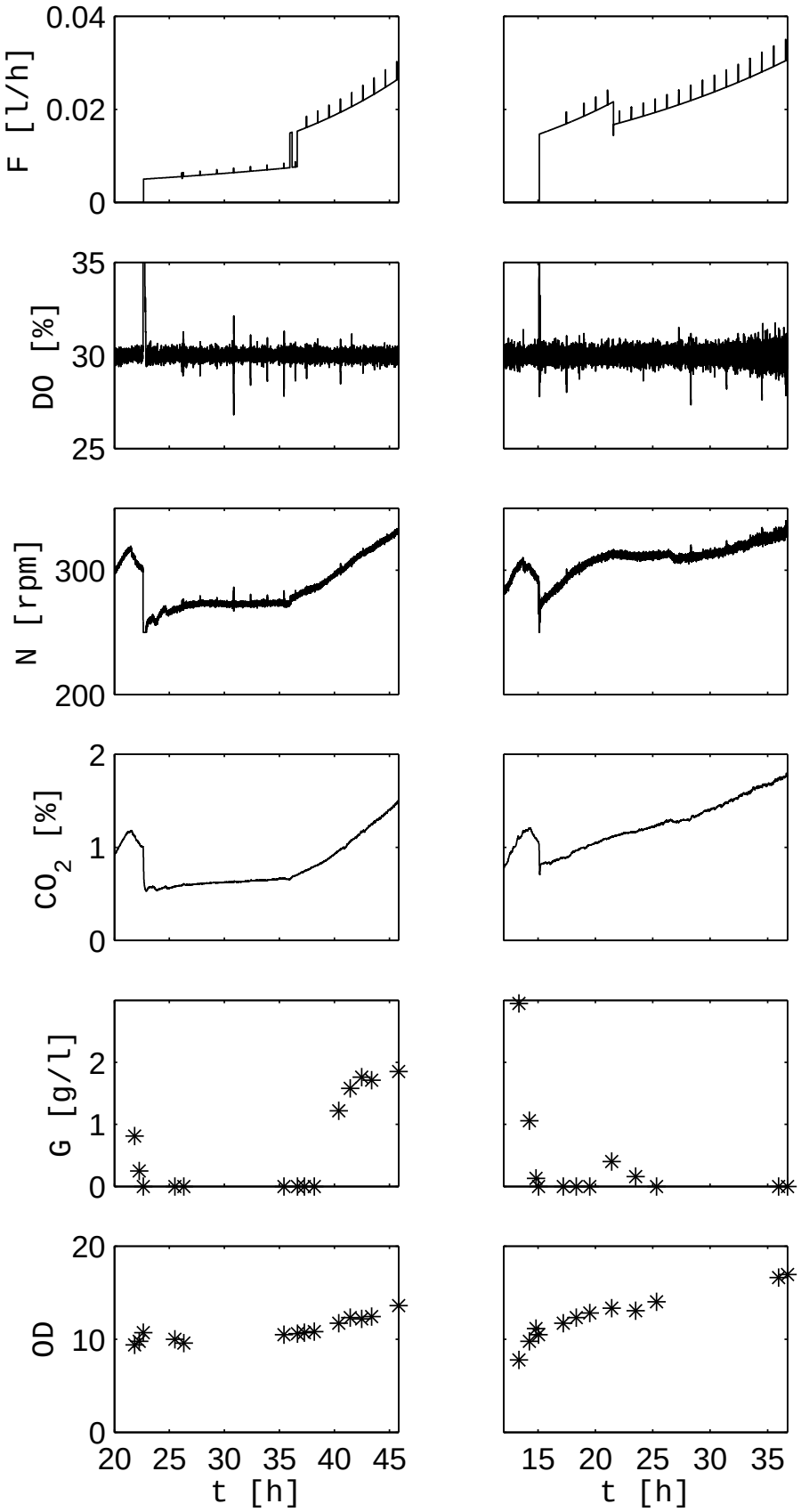

Figure 3.6 Fed-batch cultivations with exponential feed and feed pulses. To the left, the cultivation with $\mu_f = 0.03/0.06h^{-1}$, to the right, the cultivation with $\mu_f = 0.06/0.04h^{-1}$.

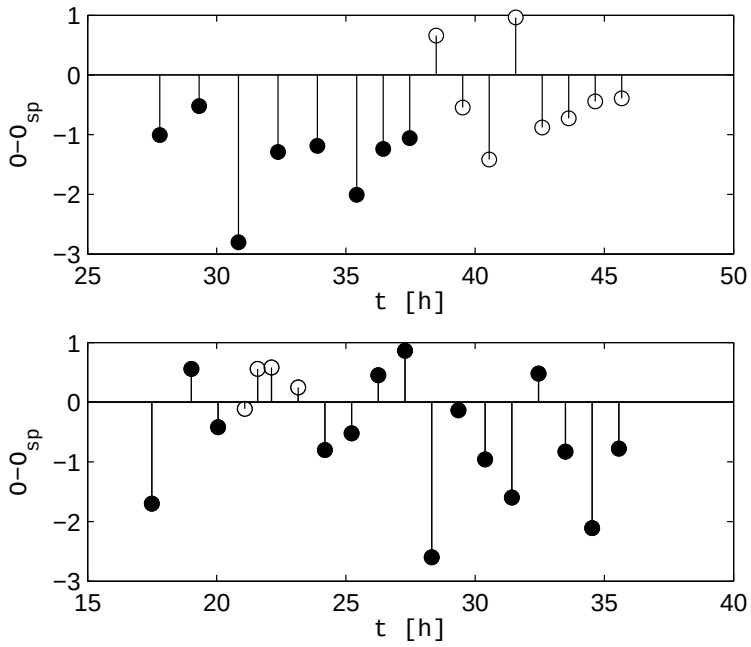

Figure 3.7 Dissolved oxygen at the end of a feed pulse from the two cultivations. White marks indicate glucose accumulation. The process noise is considerable, especially in the second cultivation.

The pulse responses in figure 3.7 is the information used for feedback in the probing control algorithm. When there is no glucose accumulation, the information from the pulse responses should be used to increase the feed rate. When there is glucose accumulation, the information from the pulse responses should be used to decrease feed rate. It is thus necessary that the reference value for the pulse response, y_r in figure 2.4 is above the average pulse response with glucose accumulation. The reference value should be close to the pulse response without glucose accumulation since the resulting feed profile should be similar to the fixed exponential feed rates in the experiments that did not lead to glucose accumulation.

The pulse responses are weak at cell densities that are as low as in these experiments. The probing controller must be tuned so that it can react on pulse responses that are this small, while being robust with respect to the process noise.

3.6 Probing Control of Fed-batch Cultivation

Conditions The batch phase was run the same way as in the previous cultivations, and with similar results. The probing feeding algorithm, as described in section 2.4, was applied with the choice of parameters in table 3.6.

These choices satisfy the stability conditions given in [1]. There, it is recommended that $O_{reac} \gg O_{tol}$. By examining the results in the previous cultivations, it can be concluded that such a choice of parameters would not be possible. The signal to noise ratio in the pulse responses is very low, but since the pulse responses are all information that is available it is necessary to rely

Parameter	*Value*
T_{pulse}	$120s$
$T_{control}$	$360s$
O_{sp}	30%
O_{tol}	0.5%
O_{reac}	0.3%
y_r	1%
γ_d	0.01
γ_p	0.15
κ	1

Table 3.1 Numerical values for parameters in probing controller

on noisy process output.

Pulse responses of magnitude O_{res} will give a feed growth rate of

$$\mu_f = \frac{\kappa(O_{res} - y_r)}{(O^* - O_{sp})(T_{pulse} + T_{control})}.$$

To achieve the feed growth rate $\mu_f = 0.06h^{-1}$, the pulse responses should on average be $O_{res} = 1.56$.

Aim In the previous fed-batch experiments, a limiting feed rate for fed-batch cultivation without glucose accumulation has been confirmed to lie in the range $\mu_f = 0.05 - 0.06h^{-1}$. The goal of this experiment is to see if the probing controller manages to avoid glucose accumulation, and if the feed rate will converge to this limiting value.

Results The result of this cultivation can be seen in figure 3.8. The batch phase does not differ from the previous cultivations. The initial feed rate was chosen rather low. During the first hour the pulse responses in the oxygen signal are large, and the feed rate is adjusted rapidly to a level that corresponds to the reference pulse response. The feed stagnates at this level for around 7 hours, after which it starts increasing at a close to exponential rate.

The responses O_{res} at the end of the feed pulses can be seen in figure 3.9. Even though there is a significant variability in the individual pulses, on average, there is a clear tendency that the pulses converge to a pulse response O_{res} just below the reference value $O_{res} = 1$. It is thus possible to use noisy measurements for the probing controller, because on average, it converges to the desired result.

No glucose accumulation can be seen during the feed phase. During the period when the feed decreases slowly, we can assume that the glucose concentration is somewhat higher in the reactor, but it is still below the level that can be detected by the instrumentation for glucose measurements.

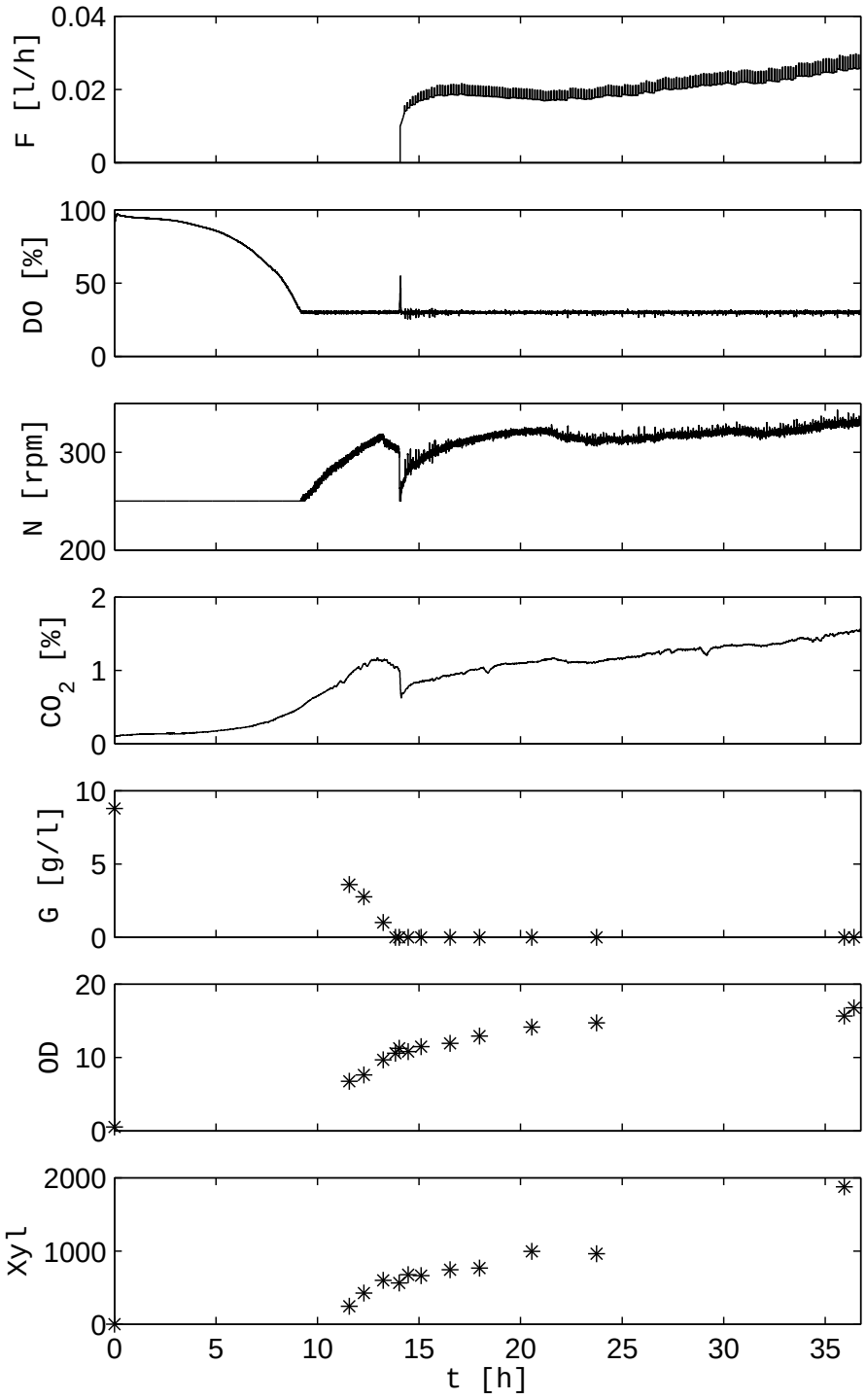

Figure 3.8 Fed-batch cultivation using probing control of the glucose feed. From top, feed rate F, dissolved oxygen DO, stirrer speed N, carbon dioxide concentration CO_2, glucose concentration G, optical density OD, xylanase activity Xyl.

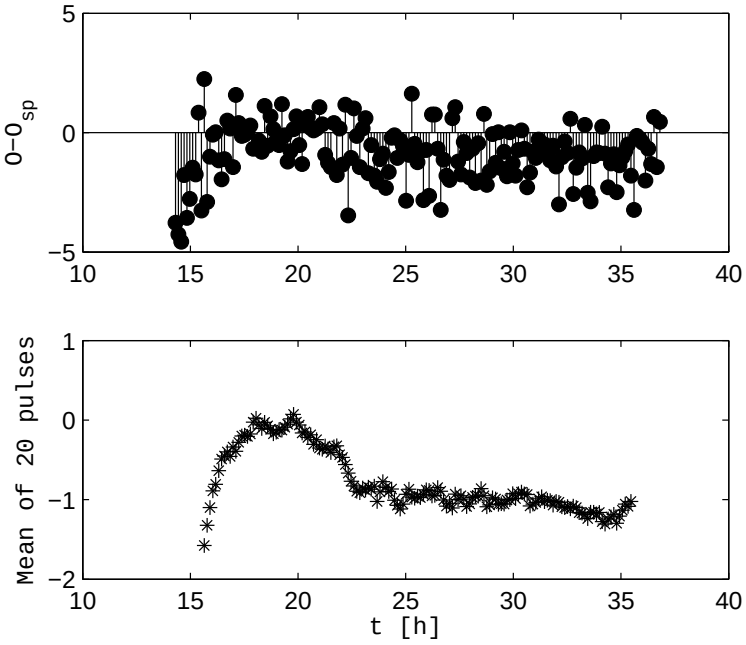

Figure 3.9 Response in dissolved oxygen on feed pulses (top), mean of 20 nearest pulses (bottom).

The cell growth rate was $\mu = 0.023h^{-1}$ in the feed phase, which matches what could be attained without glucose accumulation in the previous cultivations. After $t = 24h$, where the feed rate increases steadily, the feed growth rate was on average $\mu_f = 0.027h^{-1}$.

The probing feeding strategy manages to adjust the feed rate to a level just below what caused glucose accumulation in the previous cultivations. A comparison of the feeding strategies in all *Bacillus subtilis* fed-batch cultivations can be seen in figure 3.10.

The feed profile is similar to the cultivation where the feed increase rate was first $\mu_f = 0.06h^{-1}$ and then decreased to $\mu_f = 0.04h^{-1}$, but the probing controller decreases the feed in time to avoid the glucose accumulation seen in the previous cultivation. The feed rate increases slowly at the end of the cultivation. It is possible that the feed would have increased faster, and that the growth rate may have been marginally higher with a lower reference value y_r for the pulse responses.

Xylanase production was analyzed in this cultivation, see figure 3.8. Production starts at glucose concentrations around $G = 4g/l$, around 2 hours before the feed starts.

Conclusions The probing feeding strategy gives satisfactory results. With the goal of maximizing growth while avoiding glucose accumulation, the performance is as good as could be expected. Despite noisy process output, the feed increases steadily into an exponential profile after a transient phase.

The growth rate in the feed phase is very low, in the order of $1/10$ of the growth rate in batch phase. This substrate limiting feed strategy for fed-batch cultivation may consequently not be an optimal cultivation mode for this organism. The relation between growth rate and glucose concentration will be further discussed in the next section. From the perspective of maximizing cell

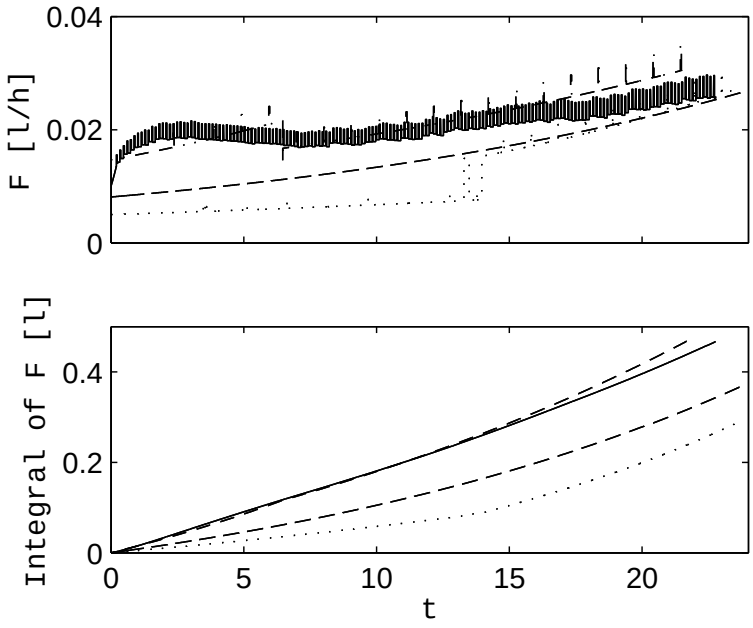

Figure 3.10 Comparison of feed strategies for the fed-batch cultivations. $\mu_f = 0.05h^{-1}$ (dashed), $\mu_f = 0.03/0.06h^{-1}$(dotted), $\mu_f = 0.06/0.04h^{-1}$ (dashed-dotted), probing feeding (solid). $t = 0$ indicates feed start. Feed rate $F[l/h]$ (top), integral of feed rate (bottom).

growth while satisfying the constraint of avoiding glucose accumulation, the cultivation run with the probing feed gives the best result of our fed-batch cultivations.

To use the probing feeding strategy, the parameters must be chosen properly. The previous cultivations gave enough information to give a reasonable choice of parameters. It is possible that the reference value y_r could be decreased somewhat, to give a faster controller so that the feed could increase more rapidly at the end of the cultivation.

4. Modelling of *Bacillus subtilis* Cultivations

A mathematical model of the dynamics of the *Bacillus subtilis* cultviations would be a useful tool for deriving good cultivation strategies and enable use of simulations for evaluation of control algorithms. A mathematical model would also be interesting on its own, presenting a compact description of all available knowledge on the organism's behavior.

The dynamics of the *Bacillus subtilis* cultivations does not match the general model presented in section 2.3. Here, an attempt to estimate some key parameters in that model will first be presented. The inconsistencies will be pointed out, and some hypotheses explaining the results will be suggested.

The data available is not sufficient for deriving a better model of the process. Further experiments, theoretical analysis, and simulations are needed for this purpose.

4.1 Parameters of Growth and Glucose Dynamics

In this section, it is assumed that the model presented in section 2.3 is accurate, and the equations in that model will be used to estimate some key parameters.

Cell Growth

Cell growth is estimated from the exponential increase rate in the carbon dioxide concentration in the outlet gas from the reactor. The measurements of cell dry weights and optical density are too few and too uncertain to provide an accurate estimate of growth. From that data, for example, it is not possible to separate lag phases from phases of exponential growth.

The estimated growth rates are shown in table 4.1. All cultivations demonstrate a period of exponential growth during the batch phase. The growth rate is consistently $\mu = 0.26h^{-1}$ during this phase. This value should correspond to a maximum growth rate. Growth in the feed phases is lower, and differs between the cultivations.

Maximum Glucose Uptake, q_g^{max}

The maximum glucose uptake q_g^{max} may be estimated from the glucose balance

$$\frac{d(VG)}{dt} = FG_{in} - q_g(G)VX.$$

At sufficiently high glucose concentrations, the glucose uptake will be approximately q_g^{max}. Thus, in the exponential batch phase whith feed $F = 0l/h$ and constant volume, the glucose dynamics will be

$$\frac{dG}{dt} = -q_g^{max}X.$$

Exponential cell growth $X = X_0e^{\mu t}$ can be assumed in this phase, with $\mu = 0.26h^{-1}$. Solving the differential equation yields

$$q_g^{max} = \frac{\mu(G(0) - G(t))}{X_0(e^{\mu t} - 1)}.$$

Cultivation	*Feed* (h^{-1})	μ_{CO_2} (h^{-1})	*Glucose*
1	batch	0.26	yes
	$\mu_f = 0.05$	0.039	-
2	batch	0.26	yes
	$\mu_f = 0.03$	0.00030	-
	$\mu_f = 0.06$	0.084	yes
3	batch	0.26	yes
	$\mu_f = 0.06$	0.019	yes
	$\mu_f = 0.04$	0.032	-
4	batch	0.25	yes
	probing	0.023	-

Table 4.1 Estimation of growth rates from carbon dioxide data

From the fed-batch cultivations, the mean maximum glucose uptake is estimated to $q_g^{max} = 0.27h^{-1}$, with standard deviation 0.052. The initial cell concentration X_0 is taken to be the dry weight at the start of the cultivation. The time t was taken to be the length of the exponential phase. Both the cell dry weight and the glucose concentration are assumed to be constant during the lag phase.

Critical Glucose Uptake, q_g^{crit}

When the glucose concentration is constant, there is an equilibrium in the glucose dynamics

$$FG_{in} - q_g(G)VX = 0.$$

The glucose uptake may be computed as

$$q_g = \frac{FG_{in}}{VX}.$$

Using the dry weight data for the cell concentration X, the glucose uptake may be estimated in the feed phases where the glucose concentration is constant. Because few dry weight measurements are available, there will be a considerable uncertainty in the estimation. The estimates in table 4.2 should however give some idea of the glucose uptake in different stages of the cultivations. In the feed phases without glucose accumulation and weak responses on feed pulses, the glucose uptake is approximately $q_g = 0.20h^{-1}$. The critical glucose uptake q_g^{crit} should be close to this value.

It is interesting to note that the difference in growth rate μ between the batch and the feed phases is much smaller than the difference in glucose uptake q_g. The low growth rate in the feed phases appears to be primarily linked to lower cell/glucose yield, rather than lower glucose uptake.

Maintenance Coefficient, q_{mc}

The cell growth rate μ is given by the equation

$$\mu = q_{gg}^{ox} Y_{xg}^{ox} + q_{gg}^{fe} Y_{xg}^{fe} + q_a^c Y_{xa}.$$

q_g (h^{-1})	*Comment*
0.076	Fed-batch cultivation with exponential feed $\mu_f = 0.03h^{-1}$, response on glucose pulses, and no cell growth
0.185	Probing controller that should give q_g just below q_g^{crit}
0.201	Fed-batch cultivation with exponential feed $\mu_f = 0.04^{-1}$, without glucose accumulation and with very weak response on glucose pulses, q_g expected to be very close to q_g^{crit}
0.215	Fed-batch cultivation with exponential feed $\mu_f = 0.06^{-1}$, a constant glucose accumulation of $G = 1.8g/l$, and without pulse respones
0.27	Estimated maximum glucose uptake q_g^{max}

Table 4.2 Estimates of glucose uptake at different stages of the cultviations

When the glucose uptake is below q_g^{crit}, no glucose is consumed by anaerobic processes, that is $q_{gg}^{fe} = 0$. Assuming low byproduct formation, these byproducts will be consumed in the beginning of the substrate limited growth, so q_a^c is assumed to be negligible over the course of the cultivation.

We then have

$$\mu = q_{gg}^{ox} Y_{xg}^{ox} = (q_g - q_{mc}) Y_{xg}^{ox}. \tag{4.1}$$

In the cultivation with exponential feed rate $\mu_f = 0.03h^{-1}$, the resultant cell growth was $\mu = 0$. All glucose was consequently used for maintenance processes, yielding $q_{mc} = q_g = 0.076h^{-1}$.

Cell dry weight / glucose yield, Y_{xg}

The cell dry weight/glucose yield in the fed-batch cultivations is shown in table 4.3. Except for the first cultivation, the yield Y_{xg} is approximately 0.30 in the batch phases.

Few dry weight measurements are available and the estimates are uncertain. It is however clear that the yield is higher in the batch phases than in feed phases. A slight increase in feed rate, from $\mu_f = 0.04h^{-1}$ to $\mu_f = 0.06h^{-1}$ with a resulting glucose accumulation also appears to increase the cell mass yield.

With the available data it is not possible to separate the oxidative yield coefficient Y_{xg}^{ox} from the fermentative yield coefficient Y_{xg}^{fe}. From the equation for the growth rate μ,

$$\mu = q_{gg}^{ox} Y_{xg}^{ox} + q_{gg}^{fe} Y_{xg}^{fe} + q_a^c Y_{xa}$$

these yield coefficients could be obtained if all measurements, all estimates, and the model in section 2.3 were accurate. Assuming negligible byproduct consumption, i.e. $q_a^c = 0$, Y_{xg} can be obtained from the fed-batch cultivations with no glucose accumulation where $q_{gg}^{fe} = 0$. When Y_{xg}^{ox} has been determined, the fermentative yield can be obtained from the stages of cultivations with glucose accumulation.

Using this method, the oxidative yield coefficient is estimated as $Y_{xg}^{ox} = 0.27$, and the fermentative yield coefficient $Y_{xg}^{fe} = 3.29$ which is clearly not a correct estimate. For comparison, we can note that the yield coefficients for *Escherichia coli* are $Y_{xg}^{ox} = 0.51$ and $Y_{xg}^{fe} = 0.15$ [10].

Cultivation	*Feed*	Y_{xg}	*Glucose*
1	batch	0.22	yes
	$\mu_f = 0.05$	0.08	-
2	batch	0.30	yes
	$\mu_f = 0.03$	0.05	-
	$\mu_f = 0.06$	0.13	yes
3	batch	0.28	yes
	$\mu_f = 0.06$	0.14	yes
	$\mu_f = 0.04$	0.05	-
4	batch	0.30	yes
	probing	0.06	-

Table 4.3 Cell dry weight / glucose yield coefficients in fed-batch cultivations.

4.2 Remaining Questions

A number of phenomena in the cultivation data and the attempt at parameter estimation in the previous section do not match the model presented in section 2.3. Some of these phenomena that are important to resolve for efficient xylanase production are discussed here. Because one phenomenon may be caused by another, they are discussed in the order they appear in the cultivations.

Increase in pH during initial lag phase

During all of the fed-batch cultivations, the pH increases during the initial lag phase. When exponential growth starts, the pH starts to decrease. The length of the lag phase and the magnitude of the increase in pH differs significantly between the cultivations.

One possible explanation for the increase in pH is that the bacteria use amino acids as a carbon source at the start of the cultivation. When amino-acids are consumed as a carbon source, pH increases. Increase in pH can also be seen when not enough glucose is available, see figure 3.2. In this case, it is natural to assume that the increase in pH is caused by consumption of some carbon source other than glucose.

At this point, no explanation for why the bacteria would initially prefer using amino acids over glucose as a carbon source has been found. Since the later parts of the cultivations do not seem to be affected by large increases in pH and long lag phases, all amino acids cannot be consumed during the lag phase.

Another possible explanation for the increase in pH is that small amounts of ammonia was leaking from the titration equipment.

Xylanase production at high glucose concentrations

Xylanase was only analyzed from the last fed-batch cultivation with the probing controller. With only one data series available, it is hard to draw general conclusions regarding under which conditions xylanase is produced.

From the xylanase data in figure 3.8 it appears that xylanase production starts around $t = 12h$, where the glucose concentration is as high as $4g/l$.

Production should be repressed in the presence of glucose, so we would not expect xylanase production before feed start. One explanation is that a limited amount of xylanase is produced even at high glucose concentrations, and the xylanase observed a few hours before feed start is a result of accumulation during the entire batch phase. If this is true, xylanase production does not appear to be at all linked to glucose concentration, since production on average is not higher in the feed-phase than in the batch-phase. Production is expected to increase with an increase in cell concentration X, and that cannot be seen in the current data.

One hypothesis for the low xylanase production at the end of the cultivation is that some byproducts are formed that inhibit production. Without analysis of byproducts, this hypothesis cannot be ruled out.

The xylanase concentration obtained at the end of the cultivation is low compared to the demands in industrial production. Analysis of xylanase activity from more cultivations is needed to draw further conclusions on xylanase production.

Change in dynamics before feed start

In all of the fed-batch cultivations, where the medium has been designed to match the needs of the cells, a sudden change in dynamics can be seen approximately 45 minutes before all glucose is consumed and the feed starts. This phenomenon for the last cultivation is shown in figure 4.1. Similar results for the other fed-batch cultivations can be seen in figures 3.5 and 3.6.

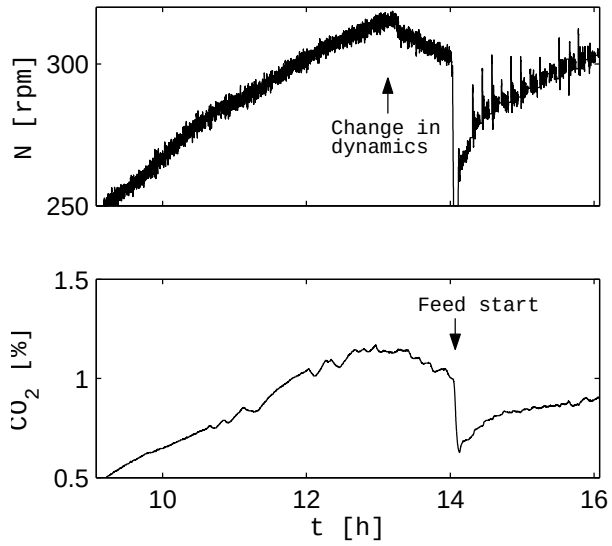

Figure 4.1 Change in dynamics approximately 45 minutes before feed start.

The decrease in carbon dioxide indicates that growth decreases. The decrease in stirrer speed indicates that the oxygen uptake decreases, which is most likely linked to a reduced glucose uptake and reduced growth rate. Different explanations have been suggested for this phenomenon.

The first hypothesis is that the medium is still not well balanced. The change in dynamics comes when some substance other than glucose is consumed. The cells must be able to function without the missing substance since growth continues during the feed phases, albeit at a much lower rate. One additional cultivation, with a higher initial glucose concentration in batch phase

would be sufficient to confirm or rule out this hypothesis. If such a change in dynamics comes at a higher glucose concentration, some substance other than glucose is limiting growth.

Another explanation that has been suggested is that ammonia used to keep pH at the set point 7 causes the change in dynamics. Titration of ammonia starts close to the end of the exponential phase. This is illustrated in figure 4.2.

Whereas ammonia could possibly cause the slow deviation from the straight line in the logarithm of the carbon dioxide, it is unlikely that it causes the very sharp decrease in stirrer speed approximately 45 minutes before feed start.

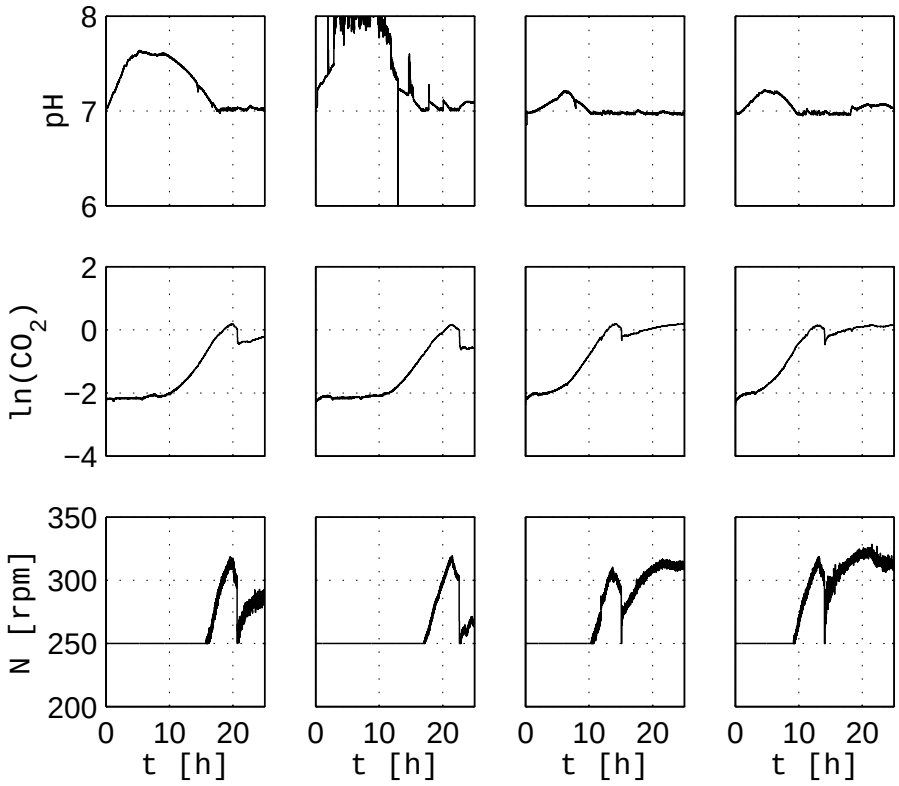

Figure 4.2 pH, logarithm of carbon dioxide, and stirrer speed for the four fed-batch cultivations. Exponential growth can be seen as a straight line in the logarithm of the carbon dioxide. It is possible that the deviation from exponential growth is linked to start of titration with ammonia that occurs when pH reaches 7.

The third explanation is that the dynamics of growth, glucose and oxygen uptake changes abruptly at a glucose concentration close to $1g/l$, a phenomenon that is not incorporated into the model in section 2.3. Growth decreases significantly at glucose concentrations below this value. This glucose concentration is not the same as the glucose concentration corresponding to the critical glucose uptake q_g^{crit}, because q_g^{crit} corresponds to the maximum glucose flow where we will see responses on feed pulses. Pulse responses cease at glucose concentration that are too low to measure, well below $G = 1g/l$ as is shown in section 3.5.

Slow growth and low cell/glucose yield in feed phase

The most noteworthy result of the fed-batch cultivations of *Bacillus subtilis* is that both growth and cell/glucose yield is significantly lower in the feed phase than in the batch phase.

If the change in dynamics before feed start discussed previously is caused by an unbalanced medium, that is the likely explanation for the slow growth and low yield in the feed phase.

If the change in dynamics is linked to the glucose concentration decreasing below $G = 1g/l$, the same change in dynamics can probably explain the slow growth and the low cell/glucose yield. It should be possible to find a new model that incorporates the change in dynamics. Such a model will differ from the model in section 2.3 with respect to how glucose flow is linked to glucose concentration. One possibility is that the Monod kinetics model that describes how glucose uptake is related to glucose concentration does not apply to this particular strain. Another possibility is that the glucose flow used for maintenance dramatically increases below a certain glucose concentration.

No analyses of byproduct formation have been made. It is thus impossible to determine how much byproducts that have been formed by anaerobic processes during the batch phases, or how much consumption of byproduct contributes to growth in the feed phases. It is possible that byproducts are formed in such high concentrations that they significantly inhibit growth.

The difference in cell/glucose yield between the batch and feed phases cannot be explained solely by the energy gain from fermentative processes since this would lead to a fermentative yield coefficient well above 1.

One hypothesis is that the growth rate decreases when xylanase production starts. This seems unlikely, however, because xylanase production is very low and appears to start before the growth rate decreases in the batch phase.

An interesting suggestion for the slow growth in the feed phase is the short period of starvation (2-3 minutes) between the moment when all glucose is consumed and the moment when the feed starts. This starvation may cause stress on bacteria that activates a number of genes that possibly changes the dynamics for a long period of time.

Process noise in response on feed pulses

The responses in dissolved oxygen on pulses in feed are noisy. On average, there is a difference in pulse responses between the case with glucose accumulation high enough to be measured, and the case with no measurable glucose accumulation. But examining the pulse responses in figures 3.7 and 3.9, it appears hard to draw conclusions regarding glucose concentration from only a single pulse.

The dissolved oxygen in the feed phase in the absence of pulses is normally distributed with mean $O = 30\%$, the setpoint, see figure 4.3. The underlying variance in the dissolved oxygen is relatively large, so large deviations in pulse responses should be expected. The noise may have many causes, e.g. air bubbles on the oxygen sensor, insufficient mixing of the medium, irregular flow from the feed pump. At low cell densities, we can expect weak pulse responses, and the signal-to-noise ratio will be low. The reference value for the oxygen response in the probing feeding cultivation was $y_r = 1$. The smaller this value is, the smaller is the average deviation from the critical glucose uptake, but decreasing y_r would put the reference pulse response within the range of underlying variation in oxygen.

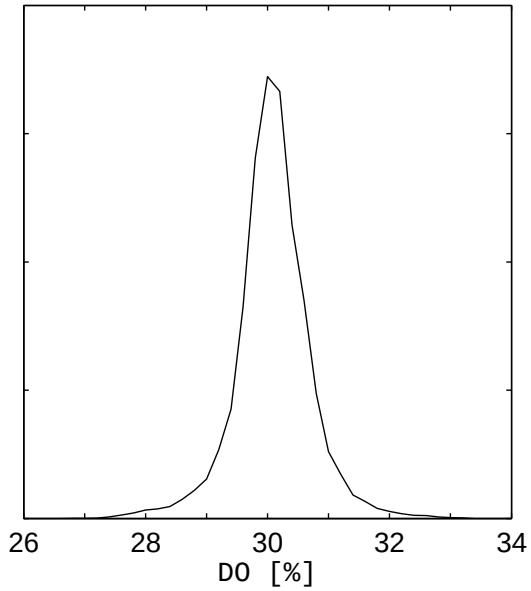

Figure 4.3 Distribution of dissolved oxygen in feed phase with exponential feed without feed pulses.

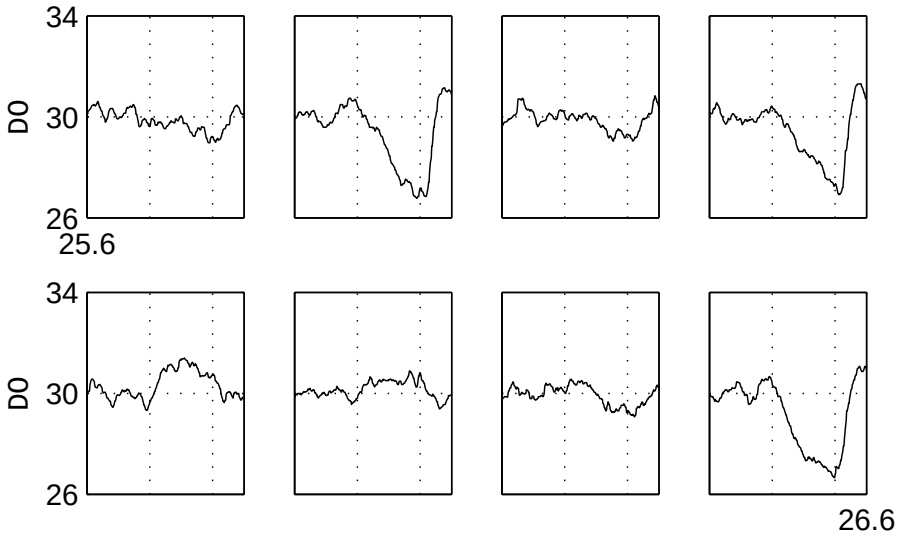

Figure 4.4 Sequence of pulse responses from fed-batch cultivation with probing control, from $t = 25.6h$ to $t = 26.6h$. The dotted vertical lines represent beginning and end of pulse. The dotted horizontal line indicates setpoint for dissolved oxygen.

In figure 4.4 a sequence of pulse responses from the fed-batch cultivation with probing control is shown. The sequence of adjacent pulses is from the middle of the feed phase, $t = 25 - 26h$, where the glucose concentration was too low to be measured. Clear pulse responses are seen for the second, fourth and eighth pulse. Almost no response can be seen in the other pulses. One explanation for why there is no response on all pulses is that the glucose uptake is sligthly above q_g^{crit} even though the glucose concentration is too low to be measured.

Because the difference in the dissolved oxygen curve is so large between the cases with clear pulse responses and the cases without any visual responses, it is likely that the great variation in pulse responses O_{res} in figure 3.9 is caused by actual variations in glucose concentration, and not only measurement noise.

5. Anti-windup for Mid-ranging Control

Mid-ranging control is a technique for using two control variables to control the same process variable. One of the control variables has fast dynamics, but is subject to saturation; the other has slow dynamics but does not suffer from the same limitations.

The oxygen transfer capacity of the bioreactor is limited. If the bacteria grow to high cell densities, the stirrer speed N will saturate, and exponential growth cannot continue. One way of solving this problem is to decrease the feed rate when N approaches the maximum value N_{max}. Decreasing F may lead to starvation, and introduces unnecessary stress on the bacteria. Another way of solving the problem is to decrease the temperature when the stirrer speed exceeds a threshold N_{ref} [10].

The activity and reproduction of the bacteria is temperature-dependent. All uptake rates $q_{(\cdot)}$ introduced in section 2.3 can be modelled as

$$q_{(\cdot)} = q_{(\cdot)}^{37} e^{-50(\frac{1}{T}-\frac{1}{37})},$$

where $q_{(\cdot)}^{37}$ is the flow rate at temperature $T = 37^oC$ [10]. As a consequence, the growth rate μ will depend on the temperature in the same way.

When the temperature decreases, the critical glucose uptake q_g^{crit} that the probing control algorithm converges to will also decrease. The algorithm will then settle for a lower optimal glucose concentration that leads to a lower oxygen uptake rate q_o. Therefore, a lower stirrer speed is needed to operate the cultivation at the critical glucose concentration. It is important to note, however, that the growth rate μ will also decrease; the temperature-decreasing approach strives for a smoother cultivation compared to the feed-decreasing approach, not a higher growth rate.

The aim of the work presented in this section is to examine whether anti-windup should be incorporated into the mid-ranging controller.

This analysis is by no means particular to *Bacillus subtilis* cultivations. Because of the lack of a good mathematical model for *Bacillus subtilis* cultivations, the general mathematical model presented in section 4 will be used for analysis, and the numerical values for the model parameters will be taken for the organism *Escherichia coli* where the dynamics is well understood.

5.1 Background

First, necessary background material on mid-ranging and anti-windup will be presented.

Mid-ranging Control

The mid-ranging controller uses two control signals, the stirrer speed N and the temperature T to control the process from a single output signal, the dissolved oxygen level O. The structure of the controller is shown in figure 5.1.

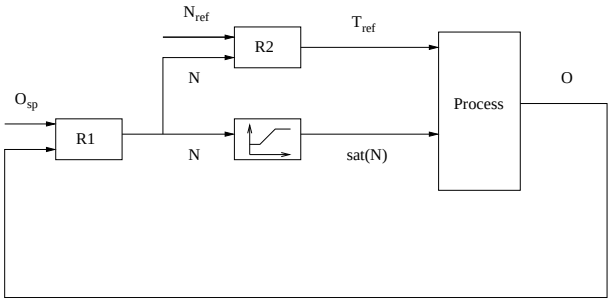

Figure 5.1 Structure of mid-ranging controller. The stirrer speed N is not allowed to decrease below a certain value, and saturates at the maximum value.

The aim of the controller is to keep the oxygen level O around the set-point O_{sp} and to adjust the temperature to keep the stirrer speed N around N_{ref}. The reference value N_{ref} should be chosen so as to make full use of the oxygen transfer capacity of the reactor.

When the control signal N exceeds N_{ref}, the temperature is reduced, which decreases the activity in the reactor, and requires a lower N to keep O at O_{sp} in steady state.

Anti-windup

Actuator saturation is a common phenomenon in control systems. The term anti-windup refers to additional static or dynamic loops in the controller that will leave the closed loop unaffected as long as the control signal does not saturate, but aim to maintain stability and performance when saturation occurs. The idea is that the controller can be designed without taking the saturation into account, and that the additional control loop limits the effects of the saturation.

In PID-controllers, saturation leads to integrator windup, where the integral term keeps increasing while the actuator is saturated and will then later over-compensate when saturation ceases. In the worst case, this windup phenomenon may lead to instability for the closed-loop system even if both the open-loop system and the closed-loop system without saturation are stable.

A common structure for a PID-controller with anti-windup is shown in figure 5.2 [2]. The difference between the input and output of the actuator is fed back to the integrator in the controller. This anti-windup scheme will be used here.

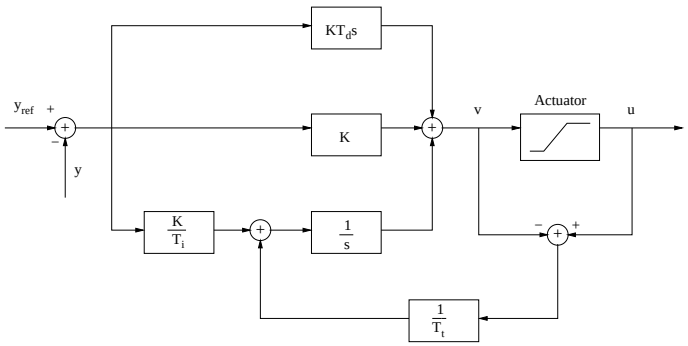

Figure 5.2 Basic anti-windup for PID-controller

5.2 Linear Model

The nonlinear model of the cultivation is defined by the equations

$$\begin{aligned}
\frac{dV}{dt} &= F \\
\frac{d(VG)}{dt} &= FG_{in} - q_g(G)VX \\
\frac{d(VA)}{dt} &= q_a(G,A)VX \\
\frac{d(VX)}{dt} &= \mu(G,A)VX \\
\frac{d(VC_0)}{dt} &= K_La(N)V(C_0^* - C_0) - q_o(G,A)VX.
\end{aligned} \tag{5.1}$$

The temperature dynamics can be approximated by a linear system

$$\frac{dT}{dt} = k_T(T_{ref} - T), \tag{5.2}$$

where T_{ref} is the reference temperature.

Plant Linearization

To facilitate analysis, this six-dimensional nonlinear model will be linearized, and only the states $O = HC_0$ and T, and the control inputs N and T_{ref} will be considered. In this analysis, it is assumed that a well-tuned feed control keeps the glucose concentration G just below the critical value, and the acetate concentration A at zero. Initially, the system is analyzed at a time-scale that is much shorter than cell growth, where the volume and cell concentration are assumed to be constant, $V = V^0$, and $X = X^0$.

The oxygen dynamics is then defined by

$$\frac{dO}{dt} = K_La(N)(O^* - O) - q_o^{37,max}e^{-50(\frac{1}{T}-\frac{1}{37})}HX^0 = F_1(O,T,N). \tag{5.3}$$

This equation is linearized around $N = N_{ref}$, $O = O_{sp}$, and $T = T^0$. The oxygen transfer coefficient K_La is modelled by a linear relation [10]

$$K_La(N) = \alpha(N - N_0).$$

The constant T^0 is chosen to give an equilibrium point in (5.3)

$$T^0 = \frac{1}{\frac{1}{37} - \frac{1}{50}\ln(\frac{\alpha(N_{ref}-N_0)(O^*-O_{sp})}{q_o^{37,max}HX^0})}.$$

The temperature dynamics

$$\frac{dT}{dt} = k_T(T_{ref} - T) = F_2(T, T_{ref})$$

gives the equilibrium point $T_{ref}^0 = T^0$.

Linearization of the differential equations for the oxygen and temperature dynamics around the equilibrium point gives the following linear system:

$$\begin{bmatrix} \frac{d\Delta O}{dt} \\ \frac{d\Delta T}{dt} \end{bmatrix} = \begin{bmatrix} \frac{\partial F_1}{\partial O} & \frac{\partial F_1}{\partial T} \\ \frac{\partial F_2}{\partial O} & \frac{\partial F_2}{\partial T} \end{bmatrix} \begin{bmatrix} \Delta O \\ \Delta T \end{bmatrix} + \begin{bmatrix} \frac{\partial F_1}{\partial N} \\ \frac{\partial F_2}{\partial N} \end{bmatrix} \Delta N + \begin{bmatrix} \frac{\partial F_1}{\partial T_{ref}} \\ \frac{\partial F_2}{\partial T_{ref}} \end{bmatrix} \Delta T_{ref}$$

with all partial derivatives taken at the equilibrium point.

From computing all partial derivatives, it follows that

$$\begin{bmatrix} \frac{d\Delta O}{dt} \\ \frac{d\Delta T}{dt} \end{bmatrix} = \begin{bmatrix} -\alpha(N_{ref} - N_0) & \frac{-50\alpha(N_{ref}-N_0)(O^*-O_{sp})}{(T^0)^2} \\ 0 & -k_T \end{bmatrix} \begin{bmatrix} \Delta O \\ \Delta T \end{bmatrix} + \\ + \begin{bmatrix} \alpha(O^* - O_{sp}) \\ 0 \end{bmatrix} \Delta N + \begin{bmatrix} 0 \\ k_T \end{bmatrix} \Delta T_{ref}. \quad (5.4)$$

In the simulations, the following numerical values of the constants in the model will be used [10]: $\alpha = 3(hrpm)^{-1}$, $N_0 = 289rpm$, $O^* = 100\%$, $O_{sp} = 30\%$, $k_T = 15h^{-1}$, $X^0 = 18g/l$. The reference value for the stirrer speed, N_{ref} will be the most important design parameter, and will consequently vary in the following discussion. To make full use of the oxygen transfer capacity of the reactor, N_{ref} should be chosen close to the maximum stirrer speed $N_{max} = 1200rpm$. With the choice $N_{ref} = 0.95N_{max}$, the following linear system is obtained:

$$\begin{bmatrix} \frac{d\Delta O}{dt} \\ \frac{d\Delta T}{dt} \end{bmatrix} = \begin{bmatrix} a_{11} & a_{12} \\ 0 & a_{22} \end{bmatrix} \begin{bmatrix} \Delta O \\ \Delta T \end{bmatrix} + \begin{bmatrix} b_{11} \\ 0 \end{bmatrix} \Delta N + \begin{bmatrix} 0 \\ b_{22} \end{bmatrix} \Delta T_{ref},$$

where $a_{11} = -2400\,h^{-1}$, $a_{12} = -5200\,\%(h^oC)^{-1}$, $a_{22} = -15\,h^{-1}$, $b_{11} = 210\,\%(hrpm)^{-1}$, and $b_{22} = 15\,h^{-1}$.

In order to use standard notation, the variables x_p and u are defined as

$$x_p := \begin{bmatrix} x_1 \\ x_2 \end{bmatrix} := \begin{bmatrix} \Delta O \\ \Delta T \end{bmatrix}, u := \begin{bmatrix} u_1 \\ u_2 \end{bmatrix} := \begin{bmatrix} \Delta N \\ \Delta T_{ref} \end{bmatrix}$$

$$y = x_1,$$

In state space form, the plant is given by

$$\frac{dx_p}{dt} = A_p x_p + B_p u \quad (5.5)$$

$$y = C_p x_p,$$

where the matrices A_p, B_p, and C_p are defined by

$$A_p = \begin{bmatrix} a_{11} & a_{12} \\ 0 & a_{22} \end{bmatrix}, \; B_p = \begin{bmatrix} b_{11} & 0 \\ 0 & b_{22} \end{bmatrix}, \; C_p = \begin{bmatrix} 1 & 0 \end{bmatrix}.$$

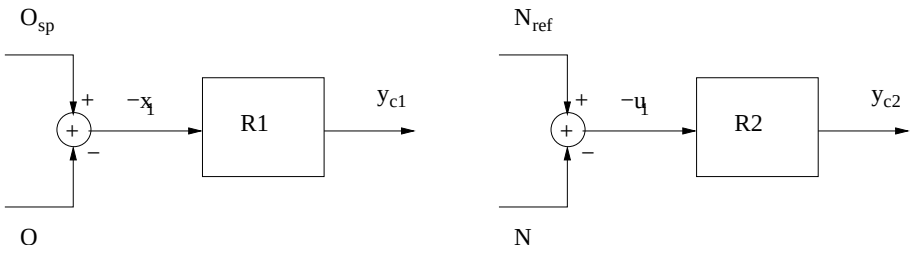

Figure 5.3 Structure of PI-controllers for stirrer speed (left) and reference temperature (right)

Controller

The controllers $R1$ and $R2$ in figure 5.1, for N and T_{ref} respectively, are both of PI-type. The input to the first controller, $R1$ is $O_{sp} - O = -\Delta O = -x_1$, and the input to the second controller $R2$ is $N_{ref} - N = -\Delta N = -u_1$.

On state space form, these controllers may be expressed as

R1:

$$\frac{dx_{c1}}{dt} = -y \tag{5.6}$$

$$y_{c1} = \frac{K_1}{T_{i1}} x_{c1} - K_1 y,$$

R2:

$$\frac{dx_{c2}}{dt} = -y_{c1} \tag{5.7}$$

$$y_{c2} = \frac{K_2}{T_{i2}} x_{c2} - K_2 y_{c1}.$$

Without saturation, the interconnected system satisfies

$$u_1 = y_{c1} \quad u_2 = y_{c2}.$$

The mid-ranging controller is designed to handle saturation of the stirrer speed, u_1. In practice the second control input, the reference temperature, is constrained to an operating range, in general around $20 - 50^oC$. From experience with both simulations and experiments, the constraints on u_2 will not severly limit performance. Therefore, only the saturation of u_1 will be incorporated in the linear model used for analysis.

The closed loop system is defined by the plant model (5.5), the controllers (5.6), (5.7), and the interconnections

$$u_1 = sat(y_{c1}), \quad u_2 = y_{c2}.$$

The function $sat(\cdot)$ is the standard saturation function:

$$sat(x) = \begin{cases} x_{min} & x < x_{min} \\ x & x_{min} \leq x \leq x_{max} \\ x_{max} & x_{max} < x. \end{cases}$$

Anti-windup

When the anti-windup scheme shown in figure 5.2 is used for the oxygen controller $R1$, the state space form of this controller will be changed according to

$$\frac{dx_{c1}}{dt} = -y + \frac{T_{i1}}{K_1 T_t}(sat(y_{c1}) - y_{c1}) \tag{5.8}$$

$$y_{c1} = \frac{K_1}{T_{i1}} x_{c1} - K_1 y.$$

When the actuator does not saturate, $sat(y_{c1}) = y_{c1}$, and the controller with anti-windup (5.8) is equivalent to the original controller (5.6).

5.3 Stability Analysis

The closed loop system with state vector $x = [x_p^T \quad x_{c1} \quad x_{c2}]^T$ is a four-dimensional piecewise affine system. The four-dimensional state space may be partitioned into three regions, $\{X_1, X_2, X_3\}$, corresponding to $u_1 = y_{c1}$, $u_1 = u_{1min}$, and $u_1 = u_{1max}$, respectively.

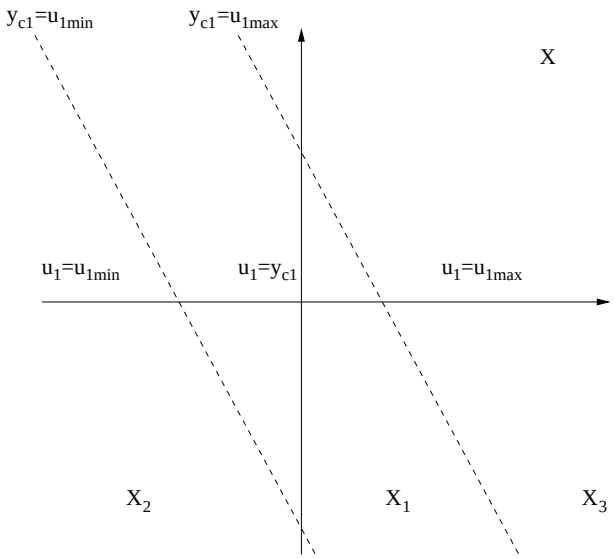

Figure 5.4 Partitioning of state space into three regions, each with affine dynamics.

Anti-windup modifies the dynamics in regions X_2 and X_3, but leaves the dynamics in X_1 unchanged. The lower bound on u_1 is applied to ensure sufficient mixing of the cultivation medium at the start of the cultivation. For the problem discussed here, the handling of oxygen transfer saturation, the lower bound on u_1 will not affect the closed loop system because the stirrer speed will operate close to the maximum value, corresponding to u_1^{max}.

In region i, $i \in \{1, 2, 3\}$, the closed loop satisfies the affine dynamics

$$\dot{x} = A_i x + a_i.$$

Expressions for the matrices A_i, a_i, A_i^{aw}, a_i^{aw} are given in appendix A.

Unsaturated System

The parameters of the PI-controllers, K and T_i, are chosen such that there is an exponentially stable equilibrium point, corresponding to $y = O - O_{sp} = 0$, $u_1 = N - N_{ref} = 0$, located in the linear region X_1. There should be no equilibrium points in X_2 or X_3; the equations

$$A_i x + a_i = 0, \quad i \in \{2, 3\}$$

do not admit solutions x_i that lie in the corresponding region, $x_i \in X_i$.

Stability of the unsaturated closed-loop system can easily be deduced from the eigenvalues of the matrix A_1. The saturated system could be analyzed using general theory for piecewise linear systems, see [5].

Saturation of Stirrer Speed

The system in figure 5.1 can be expressed in the form of figure 5.5, where the transfer function $G(s)$ includes the two controllers $R1$ and $R2$ as well as the plant P. This structure allows for stability analysis by means of absolute stability tools, such as the circle criterion [6]. This approach is easier to apply than the general theory for piecewise linear systems, but may be overly conservative since it is only a sufficient condition for stability.

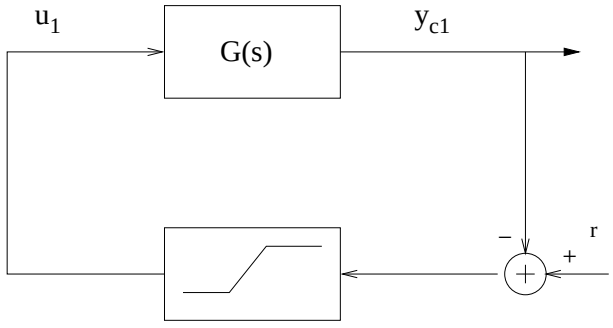

Figure 5.5 The linear system $G(s)$ with the saturation of y_{c1}.

On state space form, the system (5.5), (5.6), (5.7), can be written as

$$\dot{x} = Ax + Bu_1 \tag{5.9}$$

$$y = Cx$$

$$u_1 = -sat(y).$$

Expressions for the matrices A, B and C for the cases with and without anti-windup are given in appendix B. The reference value r in figure 5.5 is zero after linearization, in accordance with the requirements for the Cirle criterion.

The saturation function $sat(\cdot)$ is a static, time-invariant, sector-bound nonlinearity, constrained to the sector $[0, 1]$, see figure 5.6. In order to write the system on the form (5.9), it is necessary to have a precise model of the saturation, i.e. to have accurate estimates of the stirrer speed limits u_1^{max} and u_1^{min}.

From the circle criterion [6], the closed-loop system is stable for all nonlinearities in the sector $[0, \beta]$ if the Nyquist-plot of $G(s) = C(sI - A)^{-1}B$ lies to the right of the vertical line $Re[s] = -1/\beta$. The Nyquist-plots of the

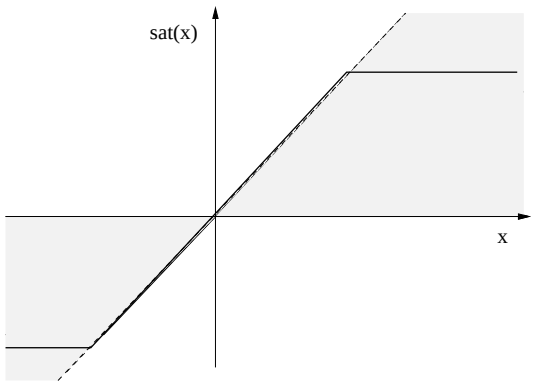

Figure 5.6 The saturation function is constrained to the sector $[0, 1]$.

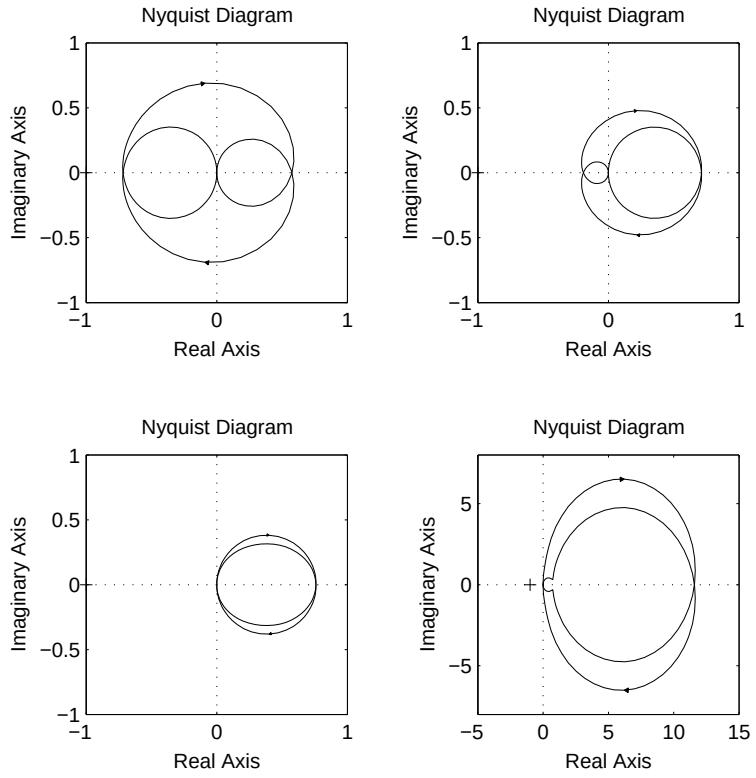

Figure 5.7 Nyquist plot of $G(s) = C(sI-A)^{-1}B$ for different choices of T_t. Upper left:$T_t = T_{i1}/3$, upper right: $T_t = T_{i1}$, lower left: $T_t = 2T_{i1}$, lower right: $T_t = \infty$ (no anti-windup).

function $G(s)$, for the case where $N_{ref} = 0.95N_{max} = 1140rpm$, $K_1 = 10$, $T_{i1} = 30/3600$, $K_2 = 0.01$, $T_{i2} = 5/60$, for different choices of the anti-windup constant T_t are shown in figure 5.7.

According to the circle criterion, the closed-loop system is stable for all examined choices of anti-windup constant T_t. The matrices A and A^{aw} are both Hurwitz, i.e. have eigenvalues with negative real part, and for stability for all nonlinearities in the sector $[0, 1]$ the Nyquist curve must lie to the right of the vertical line $Re(G(i\omega)) = -1$.

The Nyquist curves of the two systems differ considerably. Using the general

form of the circle criterion, it can be concluded that the closed-loop system is stable for saturation nonlinearities in the sector $[-1.54, 1.33]$ for the case with anti-windup constant $T_t = T_{i1}/3$, in the sector $[-1.35, 4.17]$ for $T_t = T_{i1}$, in the sector $[-1.28, 50]$ for $T_t = 2T_{i1}$, and in the sector $[-0.07, 10]$ for $T_t = \infty$, i.e. without anti-windup.

For the choice of parameters used in this section, the closed-loop system is consequently stable for a wide range of anti-windup constants T_t, when the controller output u_1 saturates according to the standard saturation nonlinearity. The ideal saturation function is constrained to the sector $[0, 1]$, but a larger sector of guaranteed stability may be desired to account for parameter uncertainty. For the case without anti-windup, the sector where the circle criterion guarantees stability was $[-0.07, 10]$, which leads to a very narrow guaranteed margin towards lower oxygen transfer than expected. By introducing anti-windup it is possible to obtain a larger sector of guaranteed stability.

Cell Growth

Different types of unmodelled dynamics affect the dissolved oxygen level, x_1. Most notably, cell growth leads to a steadily increasing demand of oxygen. The feed pulses also lead to a higher oxygen demand. Such disturbances d will be introduced in the linear model (5.5) according to

$$\frac{dx_1}{dt} = a_{11}x_1 + a_{12}x_2 + b_1u_1 + d. \tag{5.10}$$

In the Laplace domain, we have the transfer function relations:

$$\begin{aligned} U_1(s) &= R_1(s)(Y_{ref}(s) - Y(s)) = -R_1(s)Y(s) \\ U_2(s) &= R_2(s)(U_{1ref}(s) - U_1(s)) = R_1(s)R_2(s)Y(s) \\ X_2(s) &= T(s)U_2(s) = T(s)R_1(s)R_2(s)Y(s), \end{aligned}$$

where the transfer functions are given by

$$\begin{aligned} T(s) &= \frac{b_2}{s - a_{22}} \\ R_1(s) &= K_1\left(1 + \frac{1}{sT_{i1}}\right) \\ R_2(s) &= K_2\left(1 + \frac{1}{sT_{i2}}\right). \end{aligned} \tag{5.11}$$

The linearization procedure has transformed the system so that all reference signals are zero.

Without saturation of $u_1(t)$, the closed loop transfer function from the disturbance $D(s)$ to the oxygen signal $Y(s) = X_1(s)$ can be written as

$$Y(s) = \frac{1}{s - a_{11} - a_{12}T(s)R_1(s)R_2(s) + b_1R_1(s)}D(s). \tag{5.12}$$

The stationary error can be computed by the final value theorem

$$\lim_{t\to\infty} e(t) = \lim_{t\to\infty} y_{ref}(t) - y(t) = \lim_{t\to\infty} -y(t) = \lim_{s\to 0} -sY(s) = 0. \tag{5.13}$$

The cell growth may be modelled as a ramp disturbance, i.e. $d(t) = \delta t$, yielding $D(s) = \frac{\delta}{s^2}$. The stationary error is $e_\infty = 0$ for constant disturbances and ramp disturbances. For quadratic $d(t) = \delta t^2$, the stationary error is

$$e_\infty = \frac{a_{22} T_{i1} T_{i2} \delta}{a_{12} b_2 K_1 K_2},$$

and for higher degree polynomials, the error signal will be unbounded.

Without the temperature control loop, there will be a stationary error, $e_\infty = \delta T_{i1}/(b_1 K_1)$, in the dissolved oxygen signal for ramp disturbances, even without stirrer speed saturation. When the stirrer speed saturates, this error will be unbounded.

As for the case with saturation of u_1, the analysis based on the circle criterion only ensures global asymptotic stability when all inputs r and d are zero. Inputs d that are step or load disturbances could be incorporated into the system structure of figure 5.5 by adding extra states representing pure integrators. But in this case, $G(s)$ would contain poles on the imaginary axis, and the circle criterion cannot be applied to analyze stability.

5.4 Performance

Disadvantages of Anti-windup

By inspection of the Nyquist plots in the previous sections, anti-windup appears to improve robustness of the closed-loop system subject to saturation.

In the mid-ranging control setting, there are also disadvantages of anti-windup. Anti-windup aims to reduce the difference between the controller output N and the maximum stirrer speed N_{max}. In order to use the equipment efficiently, it is desirable to choose the reference for the stirrer speed N_{ref} close to N_{max}. The input to the temperature controller is the difference between N and N_{ref}, which will consequently be small for fast anti-windup (small T_t). Hence, with a fixed controller tuning, the temperature adjustment will be slower with anti-windup than without anti-windup.

This problem is illustrated by simulation in figure 5.8. The step disturbance d that increases the oxygen uptake at $t = 0.2h$ is eliminated almost instantly in the unsaturated system. The saturated system without anti-windup demonstrates the characteristic wind-up phenomenon with a large controller output that leads to an overshoot in the output O when the saturation ceases. On the other hand, the large controller output gives a fast decrease in temperature and a short period of saturation of the stirrer speed. The system with fast anti-windup, $T_t = T_{i1}/3$, avoids the overhoot in the output O, but suffers from a slow temperature decrease and a long period of saturation of N.

The mid-ranging controller is designed to handle saturation of the stirrer speed. Anti-windup is another approach for handling saturation. When the two are combined, they may interfere with a negative result on the performance of the system.

Choice of Parameters

The drawback from introducing anti-windup results from slow temperature adjustment. To counteract the effects of anti-windup, it is reasonable to in-

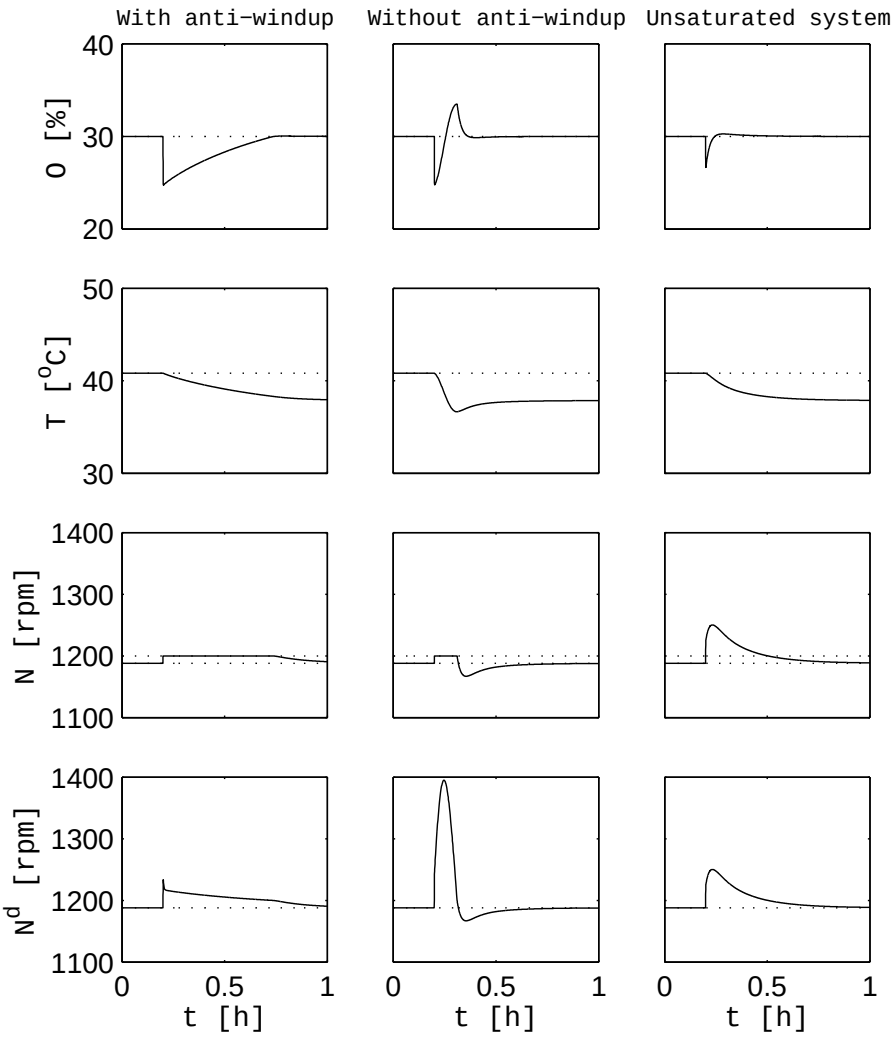

Figure 5.8 Simulation illustrating drawbacks of anti-windup for mid-ranging control. N^d denotes the output of the stirrer speed controller. The temperature decreases more slowly with anti-windup, which leads to a longer saturation of the stirrer speed, and a slower convergence of the oxygen signal.The reference N_{ref} is chosen as $N_{ref} = 0.99N_{max}$.

crease the gain and decrease the integrator time constant in the temperature controller.

However, the temperature controller must clearly be slower than the stirrer speed controller. If not, the temperature would oscillate heavily to compensate for fast oscillations in dissolved oxygen. The temperature dynamics from reference temperature to reactor temperature are too slow for such fast changes, and fast oscillations may excite unmodelled dynamics that could render the system unstable. The idea of the mid-ranging controller would be violated; the stirrer speed should be used to handle small deviations in the dissolved oxygen whereas the temperature mainly should handle the constraints imposed by cell growth. The system shown in figure 5.8 has the relation $T_{i2} = 10T_{i1}$ between the integrator time constants of the two controllers.

The effects of reducing the integrator time constant for the temperature controller is illustrated in figure 5.9. When the time constant for the slow

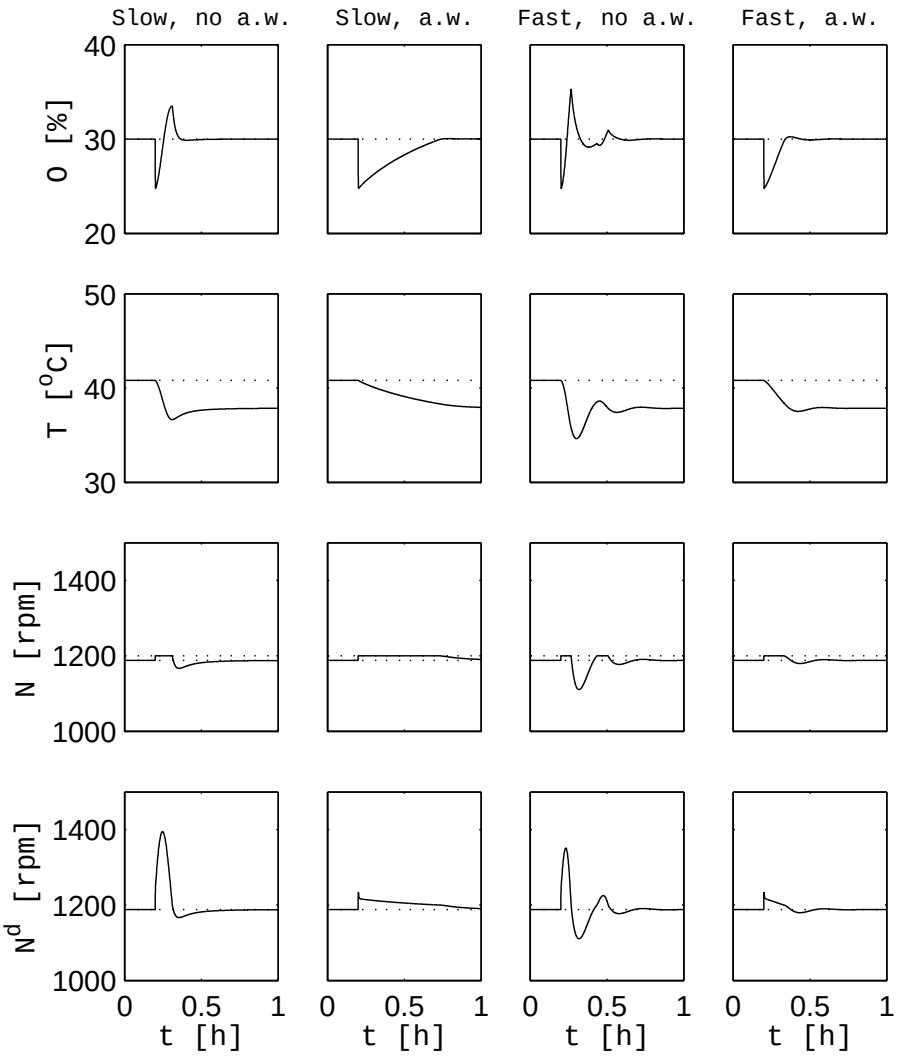

Figure 5.9 Simulation illustrating the relation between speed of temperature controller and anti-windup. First column: slow temperature controller ($T_{i2} = 10T_{i1}$) without anti-windup, second column: slow temperature controller with anti-windup ($T_t = T_{i1}/3$), third column: fast temperature controller ($T_{i2} = 2T_{i1}$) without anti-windup, fourth column: fast temperature controller with anti-windup.

controller is reduced to $T_{i2} = 2T_{i1}$, the response to a step disturbance oscillates heavily for the case without anti-windup. The response with anti-windup and a fast temperature controller avoids both the overshoot observed for the slow temperature controller without anti-windup and the slow temperature decrease obtained with slow temperature control and anti-windup.

The unsaturated system is stable for all four cases illustrated in figure 5.9. Stability of the saturated system can be guaranteed using the circle criterion for all cases except for the combination fast temperature controller and no anti-windup. For this case, the transfer function $G(s)$ in figure 5.5 is unstable, and global asymptotic stability cannot be guaranteed using this method. Saturation of u_1 implies that the stabilizing feedback loop in figure 5.5 is broken, and the unstable dynamics from u_1 to y_{c1} may dominate and render the system unstable. In the simulation in figure 5.9 the system is stable, but it

has been shown by simulation that the system can be made unstable by heavy disturbances. The other systems are robust with respect to such disturbances. It can thus be concluded that for mid-ranging control, anti-windup allows for reduction of difference in time-scale of the two controllers.

The relation between anti-windup and the speed of the slow controller in the mid-ranging control setting is summarized in table 5.1.

	Without anti-windup	*With anti-windup*
Slow temperature controller	OK	Slow system
Fast temperature controller	Stability not guaranteed	OK

Table 5.1 Effects of speed of temperature controller and anti-windup for mid-ranging control.

With the simple anti-windup scheme used here, the only parameter used for the anti-windup loop is the time constant T_t. Without anti-windup we have $T_t = \infty$, and it is generally recommended to choose T_t in the range $0.1T_{i1} - T_{i1}$ [2]. In the simulations, $T_t = T_{i1}/3$ has so far been used throughout.

The design parameters that can be chosen are the gain of the two controllers, K_1 and K_2; the time constants of the controllers T_{i1} and T_{i2}; the anti-windup constant T_t, and the reference value for the stirrer speed N_{ref}. Systematic methods for tuning these parameters, using the observations in table 5.1, would be useful, but has not been found within the scope of this thesis.

5.5 Simulations

The results in the previous section were obtained for the simplified linearized system derived in section 5.2. The conclusion, that anti-windup allows for a faster temperature controller, will here be verified by simulations of the full nonlinear system with the probing controller.

In figure 5.10, the negative effects of anti-windup can be seen. In this simulation, the time constant for the temperature controller is $T_{i2} = 5/60$, which gives a controller that is ten times slower than the stirrer speed controller. The reference value for the stirrer speed, N_{ref}, was chosen only 1% below the maximum stirrer speed $N_{max} = 1200rpm$.

Anti-windup causes the temperature dynamics to be very slow. The slow temperature dynamics leads to a long period of saturation of the stirrer speed, contrary to the purpose of anti-windup. Feed pulses are delayed until the oxygen level is within the tolerance level $O = O_{sp} \pm O_{tol}$. Therefore, in the case with anti-windup, no pulses are given when the stirrer speed saturates, and the system suffers from lack of information from feed pulses, as well as lack of control authority for a long period of time.

The system is stable both with and without anti-windup. At the end of the simulation, $t > 4h$, the system appears to approach a limit cycle. A more careful choice of parameters for the probing control may prevent this behavior.

In figure 5.11, the same system is simulated with a faster temperature controller. Here, the time constant for the temperature controller is $T_{i2} = 1/60$, which gives a controller that is half as fast as the stirrer speed controller. The

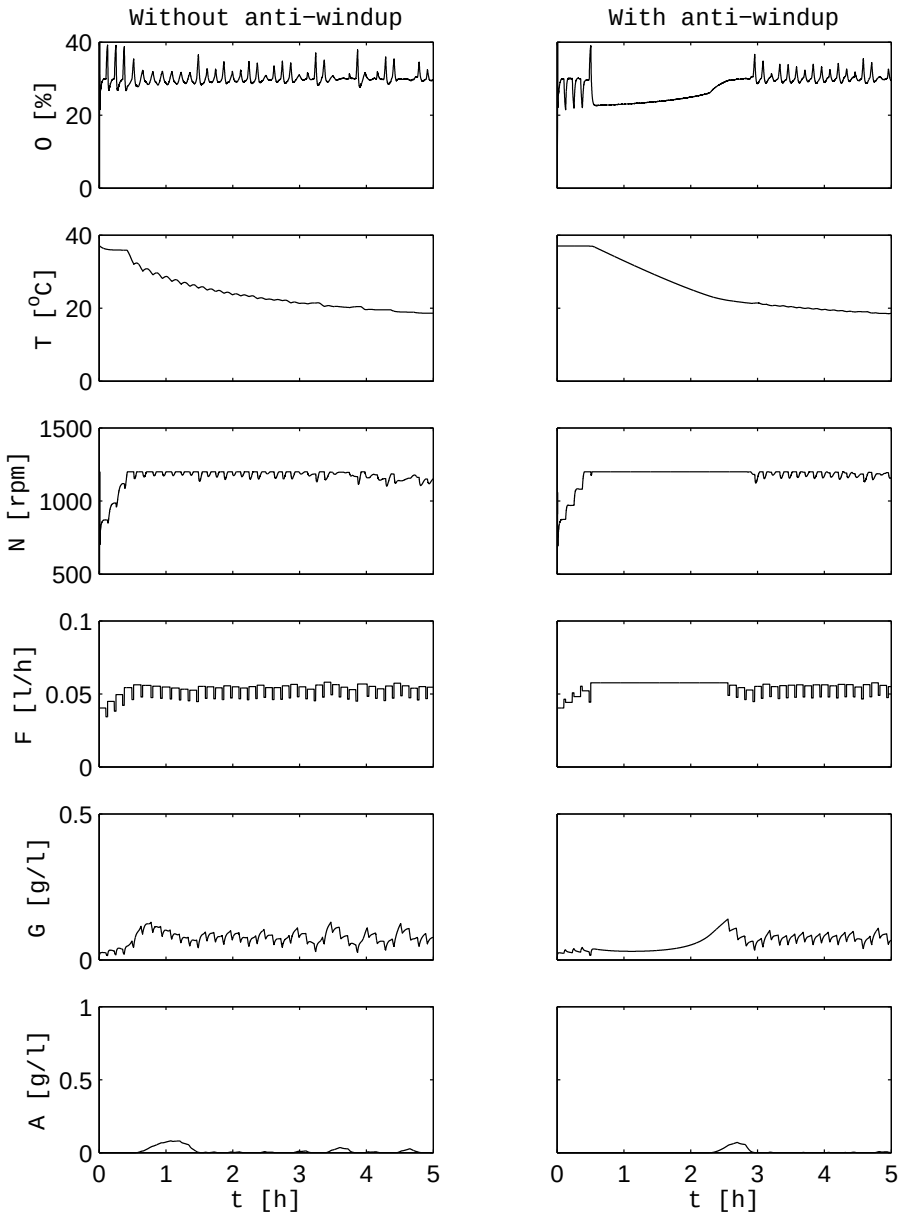

Figure 5.10 Simulation of a cultivation with (right) and without (left) anti-windup for the stirrer speed control. The time constant for the temperature controller is $T_{i2} = 10T_{i1}$.

system is unstable without anti-windup, but stable with anti-windup, and anti-windup has a clear advantage. The performance is comparable to the results obtained without anti-windup and a slow temperature controller.

The simulation results are analogous to what is predicted by the simple linear analysis, summarized in table 5.1. The additional dynamics and disturbances present in the full nonlinear system render the system with fast temperature control and no anti-windup unstable whereas the system is stable for the other cases, as predicted by the linear analysis.

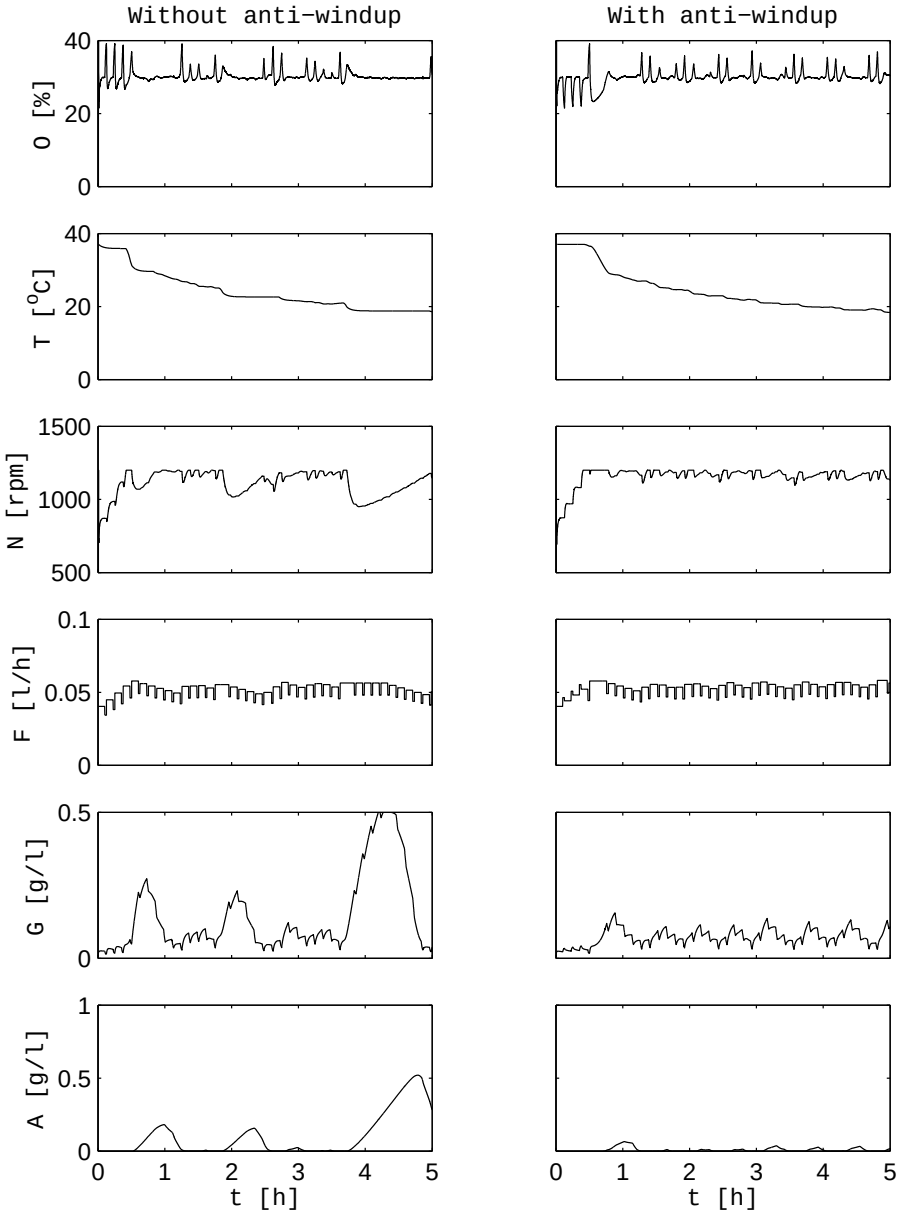

Figure 5.11 Simulation of a cultivation with and without anti-windup for the stirrer speed control. The time constant for the temperature controller is $T_{i1} = 2T_{i2}$.

6. Conclusions

The most important conclusions from the cultivations of *Bacillus subtilis* and the work on anti-windup for mid-ranging control will be discussed here.

6.1 Glucose Feeding of *Bacillus subtilis* Cultivations

The results from the cultivations do not completely match the general model when it comes to dynamics of glucose and growth. Most importantly, growth is slower and the cell/glucose yield is lower in feed phase than in batch phase. The reason for this discrepancy is still unclear, and further experiments are required to determine if the cause is lack of some component in the medium, or a more fundamental difference in the organism's glucose dynamics.

The probing feeding control algorithm has been compared to fixed exponential feed profiles. The result from using the probing feeding control is marginally better in terms of final cell density and cell/glucose yield than for the cultivations with fixed exponential feed that did not lead to glucose accumulation. The resulting feed profile resembles the feed applied in these cultivations in terms of growth rate and total amount of feed added throughout the cultivation. Consequently, under the constraint of avoiding glucose accumulation at any cost, probing feeding appears to be a reasonable control strategy. However, growth is still very slow, and the cell/glucose yield is low. Xylanase production is also rather low.

Because analyses of byproduct formation has not been made, it is not possible to draw any conclusions regarding which byproducts that are formed, and in what amounts. It is also not possible to tell how detrimental the effects of byproduct formation are on growth and xylanase production. Xylanase activity has only been analyzed from one cultivation. That data indicates that either xylanase production starts at rather high glucose concentrations, or xylanase is produced at approximately the same rate throughout the cultivation. Neither explanation matches what would be expected: negligible production in batch phase and significantly higher production in feed phase.

Avoiding glucose accumulation at any cost may not be the best cultivation strategy for *Bacillus subtilis*. If slow growth is caused by low glucose concentrations, it may be necessary to increase glucose concentration in order to obtain an acceptable growth rate. On the other hand, since xylanase production is repressed in the presence of glucose, a higher glucose concentration will decrease xylanase production. It may be necessary to separate the cultivation into two stages: first a stage with a rather high glucose concentration with relatively high growth rate, then a stage with glucose limitation where xylanase is produced. Probing control cannot be used directly for such a cultivation setup.

If the slow growth in the feed phase is caused by unbalanced medium composition, further analysis is needed in order to find the missing substance. If an appropriate medium can be found, it is likely that the probing feeding algorithm can be applied successfully to obtain a higher growth rate while avoiding glucose accumulation.

If the slow growth is caused by stress from the few minutes of glucose starvation, it is necessary to find a way to start the feed before all glucose is consumed. This can be done either manually when the measured glucose

concentration decreases below a certain value, e.g. $G = 1g/l$, or automatically by starting the feed when the decrease in stirrer speed and carbon dioxide concentration at glucose concentration approximately $G = 1g/l$ is detected. The latter approach requires that the decrease in stirrer speed is caused by a different phenomenon that does not significantly influence the results in the rest of the cultivation.

6.2 Anti-windup for Mid-ranging Control

In order to efficiently use the oxygen transfer capacity of a bioreactor, the reference value for the stirrer speed N_{ref} should be chosen close to the maximum stirrer speed N_{max}. In the mid-ranging control setting, the temperature is reduced when the output of the stirrer speed controller, N^d, exceeds the stirrer speed reference value. With a narrow margin between N_{ref} and N_{max}, it is an advantage that N^d exceeds N_{max} in order to decrease the temperature sufficiently fast.

Anti-windup aims to reduce the difference between N^d and N_{max}. Therefore, anti-windup may lead to an unnecessarily slow temperature controller, which leads to long periods of stirrer speed saturation. Anti-windup has consequently clear disadvantages in mid-ranging control.

However, the disadvantages of anti-windup may be compensated by faster dynamics in the temperature controller. With a reduced difference in time scales between the two controllers, anti-windup is required in order to guarantee stability of the saturated system, as has been shown by the circle criterion for a simplified linear system and illustrated in simulation for the full nonlinear system. Anti-windup combined with a fast temperature controller may then give results comparable with the case without anti-windup and a slow temperature controller. If a faster temperature controller is preferred in the control design, anti-windup should be considered for the mid-ranging control structure.

References

[1] Åkesson M. (1999): *Probing Control of Glucose Feeding in* Escherichia coli *Cultivations*. PhD thesis, Department of Automatic Control, Lund Institute of Technology, Lund, Sweden.

[2] Åström K.J., B. Wittenmark (1997): *Computer-Controlled Systems: Theory and Design*, 3rd Ed. Prentice Hall.

[3] Beg Q.K., M. Kapoor, L. Mahajan and, G.S. Hoondal (2001): Microbial Xylanases and their Industrial Applications: a Review, *Applied Microbiology and Biotechnology*, 56, pp. 326-338.

[4] Enfors S.O., L. Häggström (2000): *Bioprocess Technology - Fundamentals and Applications*. Högskoletryckeriet, Royal Institute of Technology, Stockholm, Sweden.

[5] Johansson M. (1999): *Piecewise Linear Control Systems*. PhD thesis, Department of Automatic Control, Lund Institute of Technology, Lund, Sweden.

[6] Khalil H. (2002): *Nonlinear Systems*, 3rd Ed. Prentice Hall.

[7] Mader S. (2004): *Biology*, 7th Ed. McGraw-Hill.

[8] Svensson U. (2004): *Fed-batch Cultivation of* Bacillus subtilis *for Xylanase Production Using Pulse Feeding with Feedback Regulation*, Master's Thesis, Department of Biotechnology, Lund Institute of Technology.

[9] Prescott L.M., J. Harley, D.A. Klein (2002): *Microbiology*, 5th Ed. McGraw-Hill.

[10] Velut S., L. de Maré, and P. Hagander (2004): A Modified Probing Feeding Strategy: Control Aspects. Technical Report, Department of Automatic Control, Lund Institute of Technology, Lund, Sweden.

A.

The piecewise affine closed-loop dynamics in regions X_i, $i = \{1, 2, 3\}$, can be expressed as

$$\dot{x} = A_i x + a_i.$$

Without anti-windup, we obtain the matrices

$$A_1 = \begin{bmatrix} A_p - K_1 B_{p1} C_p + K_1 K_2 B_{p2} C_p & \frac{K_1}{T_{i1}} B_{p1} - \frac{K_1 K_2}{T_{i1}} B_{p2} & \frac{K_2}{T_{i2}} B_{p2} \\ -C_p & 0 & 0 \\ K_1 C_p & -\frac{K_1}{T_{i1}} & 0 \end{bmatrix}$$

$$a_1 = 0$$

$$A_2 = A_3 = \begin{bmatrix} A_p + K_1 K_2 B_{p2} C & -\frac{K_1 K_2}{T_{i1}} B_{2p} & \frac{K_2}{T_{i2}} B_{p2} \\ -C_p & 0 & 0 \\ K_1 C_p & -\frac{K_1}{T_{i1}} & 0 \end{bmatrix}$$

$$a_2 = \begin{bmatrix} B_{p1} u_{1min} \\ 0 \\ 0 \end{bmatrix}$$

$$a_3 = \begin{bmatrix} B_{p1} u_{1max} \\ 0 \\ 0 \end{bmatrix}.$$

With anti-windup, we have

$$A_1^{aw} = A_1$$

$$a_1^{aw} = a_1$$

$$A_2^{aw} = A_3^{aw} = \begin{bmatrix} A_p + K_1 K_2 B_{p2} C_p & -\frac{K_1 K_2}{T_{i1}} B_{p2} & \frac{K_2}{T_{i2}} B_{p2} \\ \left(\frac{T_{i1}}{T_t} - 1\right) C_p & -\frac{1}{T_t} & 0 \\ K_1 C_p & -\frac{K_1}{T_{i1}} & 0 \end{bmatrix}$$

$$a_2^{aw} = \begin{bmatrix} B_{p1} u_{1min} \\ \frac{T_{i1}}{K_1 T_t} u_{1min} \\ 0 \end{bmatrix}$$

$$a_3^{aw} = \begin{bmatrix} B_{p1} u_{1max} \\ \frac{T_{i1}}{K_1 T_t} u_{1max} \\ 0 \end{bmatrix}.$$

B.

The system with input u_1 and output y_{c1} can be written on the form

$$\dot{x} = Ax + Bu_1$$

$$y = Cx$$

$$u_1 = -sat(y)$$

Without anti-windup, the following expressions for the system matrices are obtained

$$A = \begin{bmatrix} A_p + K_1 K_2 B_{p2} C_p & -\frac{K_1 K_2}{T_{i1}} B_{p2} & \frac{K_2}{T_{i2}} B_{p2} \\ -C_p & 0 & 0 \\ K_1 C_p & -\frac{K_1}{T_{i1}} & 0 \end{bmatrix}$$

$$B = \begin{bmatrix} B_{p1} \\ 0 \\ 0 \end{bmatrix}$$

$$C = \begin{bmatrix} K_1 C_p & -\frac{K_1}{T_{i1}} & 0 \end{bmatrix}.$$

With anti-windup, the system matrices are

$$A^{aw} = \begin{bmatrix} A_p + K_1 K_2 B_{p2} C_p & -\frac{K_1 K_2}{T_{i1}} B_{p2} & \frac{K_2}{T_{i2}} B_{p2} \\ \left(\frac{T_{i1}}{T_t} - 1\right) C_p & -\frac{1}{T_t} & 0 \\ K_1 C_p & -\frac{K_1}{T_{i1}} & 0 \end{bmatrix}$$

$$B^{aw} = \begin{bmatrix} B_{p1} \\ \frac{T_{i1}}{K_1 T_t} \\ 0 \end{bmatrix}$$

$$C^{aw} = \begin{bmatrix} K_1 C_p & -\frac{K_1}{T_{i1}} & 0 \end{bmatrix}$$